Structural architecture of the Western Alpine Ophiolites, and the Jurassic seafloor spreading tectonics of the Alpine Tethys

Journal of the Geological Society of London
(Thematic Set: "**Tethyan Ophiolites and Tethyan Seaways"**)

https://doi.org/10.1144/jgs2018-099

Structural Architecture of the Western Alpine Ophiolites, and the Jurassic Seafloor Spreading Tectonics of the Alpine Tethys

[1*]Gianni Balestro, [1]Andrea Festa, and [2]Yildirim Dilek

1: Dipartimento di Scienze della Terra, Università di Torino, Via Valperga Caluso, 35, 10125 - Torino, Italy
2: Department of Geology & Environmental Earth Science, Miami University, Oxford, OH 45056, USA

[*]**Corresponding author**:
Gianni Balestro
E-mail: gianni.balestro@unito.it
Phone: +39-011-6705865

Abstract

We present a regional synthesis of the structural architecture and tectonic evolution of the Western Alpine Ophiolites (WAO), exposed in NW Italy. The WAO represents the remnants of Alpine Tethys (Ligurian–Piedmont Ocean, LPO) that opened between Europe and Adria, and developed in four stages from Middle Jurassic to Early Cretaceous. Emplacement of gabbroic intrusions into the extending lithospheric mantle of Europe–Adria marked the main magmatic event (Stage 1). Coalescent shear zones in the fossil upper mantle (UM) form lithospheric-scale detachment faults, which led to the exhumation of UM peridotites and gabbros on the seafloor, and extensive serpentinization (Stage 2). Detachment faults, and serpentinized peridotites–gabbros in their footwalls, represent preserved fossil oceanic core complexes within the WAO. Emplacement of ophiolitic breccias and basaltic lava flows marked the syn-extensional phase (Stage 3). Radiolarian chert and limestone were deposited unconformably on this syn-extensional volcanic–sedimentary sequence, marking the post-extensional phase (Stage 4). Magmatic ages of gabbroic intrusions and mafic–felsic dykes, and depositional ages of post–extensional sequences in the WAO constrain the timing of the opening of the LPO as the Middle Jurassic (~170-168 Ma), followed by a tectonic quiescence stage in the Late Jurassic–Early Cretaceous.

Key words: Western Alpine Ophiolites; mantle exhumation; detachment fault; oceanic core complexes; seafloor spreading evolution of ophiolites; Ligurian–Piedmont ocean basin.

Introduction

The Western Alpine Ophiolites (WAO) have contributed to the ophiolite concept significantly since the 19th Century, wherein the early Alpine geologists described the spatially associated, tripartite serpentinite–diabase–chert assemblages in the Alps and Apennines as an "ophiolite", and interpreted them as ocean floor representatives for the deep axial parts of geosynclines (Brongniart, 1821; Argand, 1911; Steinmann, 1905, 1927; Elter, 1971; Bernoulli et al., 2003). Although the definition of a typical ophiolite sequence has changed considerably since these early studies (see Dilek 2003 for an overview), careful observations made by the early ophiolite geologists in the Western Alps and the Northern Apennines still remain valid. However, the WAO and their time-equivalent counterparts in the Northern Apennines (Ligurian ophiolites *s.s.*) are fundamentally different from those Penrose–type and subduction–influenced suprasubduction zone (SSZ) ophiolites, such as the Troodos (Cyprus), Semail–Oman (Oman), and Mirdita (Albania) massifs in terms of their internal structure, igneous stratigraphy, geochemical makeup and inferred emplacement mechanisms (Decandia & Elter, 1972; Dilek et al. 1990; Tankut et al., 1998; Dilek & Flower, 2003; Dilek et al., 2007; Dilek & Furnes 2009, 2014; Dilek & Thy, 2009; Pearce & Robinson 2010; Goodenough et al. 2014; Piccardo et al., 2014; Saccani et al., 2015, 2018; Capponi et al., 2018). The WAO and the Ligurian ophiolites were derived from the oceanic lithosphere of the Liguria–Piedmont Ocean, whereas the SSZ ophiolites in the Neotethyan realm to the east were originated from the upper plate of a subduction zone within Neotethys (Dilek 2003; Dilek & Robinson, 2003; Dilek & Furnes, 2011, and references therein). Therefore, the WAO provide a unique opportunity to examine in 4-dimensions the structure and stratigraphy of a fossil, subduction–unrelated oceanic lithosphere (sensu Dilek & Furnes 2011), and to investigate the seafloor spreading tectonics of an embryonic ocean basin.

In this paper, we present new structural and lithostratigraphic observations from the WAO exposed in the Western Alps, synthesize the available geochronological (i.e., U–Pb dating of zircons) and biostratigraphical (i.e., radiolarian ages) information on these ophiolites in the extant

literature. We also present a comprehensive model for a multi–phase development of the WAO and the seafloor spreading evolution of the LPO. Our work in the WAO has focused on a systematic, comparative documentation of the internal structure and lithostratigraphy of main ophiolite complexes, in which we identified remnants of key stratigraphic unconformities and major oceanic shear zones that are reminiscent of those documented for detachment faults from in situ oceanic core complexes along the slow-spreading Mid-Atlantic and Southwest Indian Ridges (Karson and Dick, 1983; Blackman et al., 1998; Tucholke et al., 1998; Escartin et al., 2003, 2017; Boschi et al., 2006; Cannat et al., 2006; Ildefonse et al., 2007; Miranda & Dilek, 2010; Bonnemains et al., 2017). Using these key structures and their timing of development, we have reconstructed a common architecture of the ophiolites that reflects their pre–alpine evolution. The reconstructed structure and stratigraphy of the WAO and our interpretation of the evolution of the LPO, involving the seafloor spreading of a restricted ocean basin and post-extensional deposition stages, took ~25–30 million years between the Middle Jurassic (~170-168 Ma) and the tectonic quiescence in the Late Jurassic - Early Cretaceous.

Regional Geology of the Western Alpine Ophiolites

The Alpine orogenic belt developed as a result of the collision between Adria in the upper plate and Europe in the lower plate as the intervening LPO (Alpine Tethys) closed in the Early Cenozoic (Dal Piaz et al., 1972; Ricou & Siddans, 1986; Coward & Dietrich 1989; Laubscher 1991; Dilek, 2006; Handy et al., 2010). The LPO evolved after the Late Triassic – Early Jurassic rifting between these two continents, followed by the Middle to Late Jurassic seafloor spreading. It has been widely interpreted as an ocean basin, floored by hyper–extended crust and exhumed lithospheric mantle that underwent low degrees of partial melting during slow spreading (Lemoine et al., 1987; Michard et al., 1996; Lavier & Manatschal, 2006; Manatschal & Muntener, 2009; Saccani et al., 2015). The geochemical makeup of the Western Alpine and coeval Northern Apennine ophiolites is well documented in the literature (Piccardo & Guarnieri, 2010, and the references

therein). Our study here does not involve this aspect of the WAO, but we have utilized the widely accepted petrogenetic interpretations and models for their melt and magmatic evolution.

It is generally accepted that the subsequent Alpine orogeny included the following tectonic stages: (*1*) Late Cretaceous to Middle Eocene subduction, (*2*) Late Eocene to Early Oligocene continental collision, and (*3*) Late Oligocene to Neogene deep crust/mantle indentation and development of a doubly-verging crustal architecture (Steck & Hunziker, 1984; Platt et al. 1989; Polino et al. 1990; Stampfli & Marthaler, 1990; Michard et al., 1996; Rosenbaum & Lister, 2005; Dilek, 2006; Butler et al. 2013; Festa et al., 2019).

Remnants of the LPO (Dal Piaz et al., 2003) contain eclogite-facies (i.e., Zermatt Zone) and blueschist-facies tectonic units (i.e., Combin Zone) that mark the suture zone between Europe and Adria (Figs. 1A and 1B; Bearth, 1967; Ballèvre et al, 1990; Ballèvre and Merle, 1993; Balestro et al., 2009; Tartarotti et al., 2017). Some researchers consider the WAO as the remnants of an embryonic ocean (Pognante et al., 1986; Lombardo et al., 2002), whereas some others as the lithospheric fragments of a magma poor ocean-continent transition zone of the Alpine Neotethys (Froitzheim and Manatschal, 1996; Manatschal and Bernoulli, 1999; Manatschal, 2004).

In the study area (Fig. 2), the WAO are represented by three ophiolite complexes (Monviso - MO, Queyras Schistes Lustrés - QU, and Chenaillet - CH), which display different Alpine metamorphic overprint and deformation features. The MO is N-S–trending, few km-thick (Fig. 2) and extends for ~35 kilometres along strike (Balestro et al., 2018). It is tectonically juxtaposed against the Dora Maira Unit, which represents part of the deeply subducted and exhumed continental margin of Europe. The MO consists of serpentinite, metagabbro, metabasalt and metasedimentary rocks (Lombardo et al., 1978). The general structure of the MO is a manifestation of subduction zone deformation and metamorphism (eclogite-facies), and subsequent collision related, W-vergent folding and shearing, coeval with blueschist- and greenschist-facies metamorphic re-equilibration (Philippot, 1990; Groppo & Castelli, 2010; Angiboust et al., 2012; Balestro et al., 2014; Balestro et

al., 2015b). However, the primary lithological units, their contact relationships, and the seafloor spreading–related structures are overall well preserved in the MO.

The QU to the west overlies the MO tectonically (Fig. 2) and consists of three major units (the lower, intermediate and upper units of Lagabrielle & Polino, 1988) that were juxtaposed together during the continental collision-related alpine–stage shortening, associated with large-scale boudinage development and pervasive folding. The QU is made of blocks of serpentinized metaperidotites, metamorphosed gabbros and metabasaltic lavas, all of which are embedded in a metasedimentary unit (Schistes Lustrés Auct.; Lemoine & Tricart, 1986; Lagabrielle & Polino, 1988; Deville et al., 1992). Blocks of these lithologies range in size from a few metres to few kilometres. Metasedimentary succession is composed of metabreccia with mafic–ultramafic rock clasts, metachert, marble and widespread calcschist (Tricart & Lemoine, 1991; Tricart & Schwartz, 2006). Both the blocks and their meta-sedimentary matrix display alpine-stage blueschist metamorphic overprint, whose degree decreases structurally up–section within the QU (Vitale Brovarone et al., 2014).

The CH in the west constitutes a <1 km–thick thrust sheet, juxtaposed against the QU (Fig. 2; Lemoine, 1971; Bertrand et al, 1987; Manatschal et al., 2011). It consists of serpentinized peridotites intruded by small gabbroic plutons and stocks (up to 200 metres wide) and covered by few m–thick, discontinuous layers of clastic sediments derived from an ophiolitic source, and up–to 400-m-thick basaltic lavas (Caby, 1995; Chalot Pra, 2005). It displays sub-greenschist facies metamorphic mineral assemblages and textures, and hence it is the least metamorphosed LPO remnant among the WAO (Mével et al., 1978).

Internal Structure and Stratigraphy of the Western Alpine Ophiolites

In this section, we describe and document the intraoceanic (i.e., pre-Alpine) internal structure and stratigraphy of the Monviso (MO), Queyras (QU) and Chenaillet (CH) ophiolites, with a focus on

their lithological units, contact relationships (intrusive, tectonic, unconformity), and mineral assemblages and textures. Primary intra-oceanic features and internal organization are constrained, for the first time in this paper, through a correlation of regional-scale stratigraphic unconformities, previously recognized in the MO by Balestro et al. (2015b) and Festa et al. (2015). These unconformities are defined as primary depositional surfaces; the lack of any deformational structures and mylonitic textures associated with them indicates that they do not represent shear zones or fault contacts. Unconformities allow us to recognize stratigraphic breaks in the depositional records of ocean basin strata (see, e.g., Clari et al., 1995 and reference therein).

We have identified three major tectonostratigraphic sequences within the WAO, marking significant temporal boundaries in the pre–alpine evolution of the LPO. These tectonostratigraphic sequences include: serpentinized upper mantle (UM) metaperidotites with mafic to felsic meta-intrusive rocks, a syn–extensional metavolcanic and metasedimentary succession, and a post–extensional metasedimentary succession. Extensional mylonitic to cataclastic shear zones with talcschist and serpentine schist assemblages make up the top structural horizon of the UM metaperidotites, and are hereby interpreted as oceanic detachment faults. The syn–extensional metavolcanic and metasedimentary succession with a syn–kinematic ophiolitic metabreccia rests directly on these shear zones. The youngest post–extensional sedimentary succession on top contains different lithofacies distribution than the other two, older sequences.

In our descriptions of the lithological units and their ages we use the geological time scale of the International Chronostratigraphic Chart by Cohen et al. (2018).

Monviso Ophiolite (MO)

The MO represents the structurally lowest ophiolite complex within the present-day tectonic stack of the WAO (Figs. 2, 3A and 3B), and displays the highest degree of alpine–stage deformation and metamorphism among the three ophiolite complexes.

Upper mantle peridotites and mafic and felsic intrusions

The UM metaperidotites in the MO are represented largely by up to 1 kilometre–thick, massive serpentinite. Weakly serpentinized domains within this UM sequence consist of metalherzolite and metaharzburgite, with strongly deformed porphyroclasts of olivine, orthopyroxene and clinopyroxene. Locally preserved lizardite with mesh structures suggests primary ocean floor serpentinization, which likely occurred at temperatures below 300°C (Lafay et al., 2013). Massive serpentinite outcrops are directly overlain by metres-thick, discontinuous layers of meta-ophicarbonate (Fig. 3A).

Metagabbros occur as intrusive bodies in the massive serpentinites (Fig. 3A) and range in size from decimetres–thick dykes to 100s of metres–thick and sub-kilometre long stocks and plutons. Their emplacement age has been constrained to 163±2 Ma (i.e., middle Callovian–early Oxfordian; Rubatto & Hermann, 2003). Gabbroic rocks are composed mainly of Mg- and Al-rich and minor Fe and Ti-rich metagabbros. Mg- and Al-rich metagabbro is medium- to coarse-grained, and includes augite mostly replaced by Cr-bearing omphacite, plagioclase replaced by clinozoisite and albite, and rare chromite and ilmenite. Olivine bearing metagabbro and cumulate metatroctolite are locally associated with Mg- and Al-rich metagabbro. Fe- and Ti-rich metagabbro occurs as pods within the Mg- and Al-rich metagabbro outcrops (Fig. 3A), and consists of garnet, omphacite, rutile and relics of augite. Augite grains show hornblende intergrowths with low $\delta^{18}O$ values, produced by hydrothermal alteration of gabbro (Rubatto & Angiboust, 2015). Contacts between the massive serpentinite and metagabbro are marked by rodingitic reaction rinds, composed of grossular garnet, Mg-chlorite, epidote, diopside and vesuvianite. Locally, the lack of pervasive alpine metamorphic overprint (Bogatto & Castelli, 1997) indicates that the rodingite forming metasomatic event started as part of an *in-situ* oceanic serpentinization process.

Massive serpentinite and metagabbro bodies were both intruded by felsic dykes (Fig. 3A). A 152±2 Ma (i.e., Middle Kimmerdigian to Early Tithonian; see Lombardo et al., 2002) lenticular body of Fe-rich metaquartzdiorite (several tens of metres-wide) is also intrusive into an Fe- and Ti-rich

metagabbro along sharp, chilled margins. Metaplagiogranite intrusions in the serpentinite are transformed into jadeitite with omphacitite as a result of a late-stage metasomatic overprint (Compagnoni et al., 2012). A decimetres–thick meta-albitite dyke in a metabasalt host (Fig. 4A) consists of quartz and albite, amphibole and white mica aggregates. These 152±2 Ma felsic dykes are the products of a late-stage intraoceanic magmatism.

The exposed, uppermost surface of the massive serpentinite unit in the MO locally displays up to few tens of metres–thick talcschist and serpentine schist (Fig. 4B). Talcschist comprises talc, chlorite and amphibole, with minor calcite, magnetite, garnet and apatite, whereas the serpentine schist consists mainly of antigorite and magnetite with minor talc and calcite. These schistose rocks also include decimetres to metres-long blocks of Fe- and Ti-rich metagabbro (Fig. 3A). Unlike the metagabbro bodies within the massive serpentinite, these metagabbro units are devoid of rodingitic reaction rims, indicating that their emplacement must have occurred after the main phase of intraoceanic serpentinization of the UM peridotites. Some metagabbro blocks are enveloped by up to decimetres–thick cataclastic metabreccias, which are composed of the same gabbroic rocks as in the blocks. Talcschist and serpentine schist rocks with cataclastically deformed metagabbros, forming tectonic breccias, have been interpreted as the products of intraoceanic, pre-alpine detachment faulting (i.e., the Baracun Shear Zone of Festa et al., 2015), which involved rock-fluid interactions among gabbro intrusions, serpentinite and hydrothermal fluids during the exhumation of the lithospheric mantle.

Syn-extensional volcanic and sedimentary sequence

The massive serpentinite and metagabbros, and the serpentine schist– and talcschist–bearing shear zone (Fig 3A), are discontinuously overlain by metabasaltic lavas and calcschist with metasandstone and metabreccia interlayers (Fig. 3A). Metabasaltic lavas (Fig. 4A) range in thickness from tens of metres to several hundreds of metres, and include fine-grained aphyric metabasalt, pillow metalavas (up to 1 m in size), and volcanic metabreccia. These mafic metalavas

are composed mainly of albite, amphibole, chlorite and epidote with relics of garnet and omphacite. Minor amounts of white mica, carbonate and quartz occur in the volcanic metabreccia. Rare centimetres thick layers of quartzite (i.e., the very bottom of the post-extensional sequence, see below) occur at the top of this volcanic metabreccia. Metabasaltic rocks also occur as decimetres-thick, fine-grained dykes within the metagabbro bodies.

Calcschist in the syn-extensional stratigraphic units mainly consists of calcite, quartz, Mg–chlorite and Cr–bearing white mica, and contains magnetite pseudomorph after spinel. Metasandstone and matrix-supported (sedimentary) metabreccia interlayers (Fig. 4C) within the calcschist are made of sub-angular clasts of metagabbro, which consists of omphacite, chlorite, Cr-bearing white mica and epidote. Metasandstone shows graded-bedding and metabreccia laterally grades into metasandstone in some outcrops. Thickness of the calcschist shows significant lateral variations, ranging from several centimetres to ~70 metres (Balestro et al., 2015b), and generally tapers out towards the sheared horizons of talcschist and serpentine schist of the Baracun Shear Zone (Figs. 3A and 3B).

Post-extensional sedimentary sequence

The ophiolitic units and the syn-extensional cover of the MO are unconformably overlain by thin (~several decimetres-thick) horizons of whitish marble that are in turn unconformably overlain by several tens of metres-thick calcschist (Fig. 3A). The whitish marble (Fig. 4D) consists of calcite and white mica, and it closely resembles the Upper Jurassic–Lower Cretaceous Calpionella Limestone of the non-metamorphosed cover of the Internal Ligurian ophiolites in the Northern Apennines (Fig. 4B). The calcschist contains distinct, few centimetres to several decimetres thick horizons of impure marble and quartz schist (Fig. 4B).

This post–extensional calcschist is devoid of any ophiolite derived detrital material, although it unconformably overlies the ophiolite units and the syn-extensional sequence. It mainly contains carbonate minerals, quartz and white mica, whereas the quartz schist interlayers include quartz,

white mica and chlorite with minor albite and garnet. The age of the post-extensional calcschist was interpreted as the Early Cretaceous (Lagabrielle, 1994), based on its correlation with a package of similar unmetamorphosed sedimentary rocks (e.g., Palombini Shale) in the Northern Apennines.

Queyras Ophiolite (QU)

QU is tectonically juxtaposed against the MO to the east, and consists of tectonically sliced remnants of ophiolite units and related metasedimentary cover successions (Figs. 5A and 5B). Ophiolitic lithologies include serpentinized metaperidotites, metagabbros and metabasalts.

Upper mantle peridotites and mafic-felsic intrusions

Serpentinized metaperidotites in the QU consist of plagioclase-bearing lherzolite with minor harzburgite, dunite and pyroxenite, and locally retain lizardite mesh textures (Schwartz et al., 2013). As in the MO, the serpentinized peridotites in the QU are also capped by both massive and sheared meta-ophicarbonate horizons, which are locally up to few tens of metres in thickness (Fig. 5A).

The metaperidotites are intruded by dykes and stocks of metagabbro (Fig. 5A). Gabbroic rocks are commonly coarse-grained and rodingitized, and locally display pegmatitic textures. They have Mg- and Al-rich compositions and consist of albite, zoisite, chlorite, epidote, Na-bearing amphibole, jadeite, garnet and phengite, with relict porphyroclasts of olivine and augite with hornblende rims. Locally well preserved mylonitic to flaser textures in the metagabbros represent pre-alpine, intra-oceanic deformation fabrics (Lagabrielle, 1987).

Fe- and Ti-rich metagabbro in the serpentinized metaperidotites is spatially associated with Mg- and Al-rich metagabbro bodies (Fig. 5A), and forms up to tens of metres-long lenticular bodies or irregular pods. These metagabbros consist mainly of clinopyroxene, widely replaced by amphibole and chlorite, and albite, chlorite and epidote pseudomorphs after plagioclase, and ilmenite replaced by Fe-oxide and titanite. Felsic meta-intrusive rocks vary from metaleucodiorite to meta-albitite, metatrondjemite and metaplagiogranite *s.s.* (Lombardo & Pognante, 1982; Carpena &

Caby, 1984), forming few decimetres-thick dykes. Metamorphic mineral assemblages in these dyke rocks include albite, quartz, jadeite and amphibole. Fine-grained, hypabyssal metadolerite locally overlies the metagabbro.

Similar to the MO, up to 20-metres-thick, discontinuous layers of talc and chlorite schist, serpentine schist and chloritite (Fig. 6A) occur at the top of massive serpentinites (Fig. 5). These rocks locally include blocks of metagabbro (Pinet et al., 1989), and display mylonitic to cataclastic shear zones (Lagabrielle et al., 2015). The uppermost part of massive serpentinites also includes Cu- and Fe-sulphide mineralization zones, interpreted to be exhalative deposits formed as a result of hydrothermal discharge on the seafloor (Giacometti et al., 2014).

Syn-extensional sedimentary and volcanic sequence

The oldest sedimentary rocks resting directly on the serpentinized metaperidotites, metagabbro bodies and shear zones, are laterally discontinuous and consist of few centimetres- to several tens of metres-thick layers of polygenic metabreccia and metasandstone (Fig. 5A). These rocks are poorly sorted and matrix-supported, and have centimetres scale sub-angular clasts (Fig. 6B), which are made of metaperidotite, serpentinite, metagabbro and metaflasergabbro, with minor occurrences of basaltic, quartz and feldspathic clasts (Tricart & Lemoine, 1983; Le Mer et al., 1986). The matrix is composed of very fine-grained carbonate, amphibole, chlorite, epidote, albite and antigorite assemblages. These polygenic metabreccia and metasandstone units are locally overlain or interfingered with a metabasalt sequence, which consists of metapillow lavas and basaltic (monogenic) metabreccias, ranging in thickness from few metres to 200 metres (Fig. 6C). Monogenic metabreccia clasts are angular to irregular in shape, up to 30 centimetres–wide, and embedded in a matrix of chlorite, albite, epidote, amphibole, white mica and calcite (Lagabrielle & Polino, 1985). Fine-grained, decimetre–scale metabasaltic dykes crosscut the serpentinite, metagabbro and metaflasergabbro (Lombardo & Pognante, 1982; Tricart & Lemoine, 1983). Locally,

metadolerite dykes crosscut the metagabbro and metaflasergabbro units, and a metabreccia unit containing doleritic clasts overlies the metagabbro (Saby, 1987; Pinet et al., 1989).

Post-extensional sedimentary sequence

The ophiolitic units and the syn-extensional metasedimentary and metavolcanic sequences of the QU are unconformably overlain by a post-extensional metasedimentary sequence (Fig. 5A). The latter starts at the bottom with a Middle to Upper Jurassic metachert unit, which is overlain along a regional-scale unconformity by an Upper Jurassic to Lower Cretaceous whitish marble unit (Fig. 5A). Discontinuous layers of metachert rest unconformably on meta-ophicarbonate and metabasalt (Figs. 5B and 6D), or occur as local intercalations within basaltic metabreccia. The metachert consists mainly of quartz and Fe- and Mn-oxides, and may contain in places Middle Bathonian (Unitary Association Zone, UAZ 6 of Baumgartner et al., 1995; Cordey & Bailly, 2007), Upper Bathonian to Lower Callovian (UAZ 7 of Baumgartner et al., 1995; Schaaf et al., 1985; De Wever et al., 1987) and Upper Oxfordian (UAZ 9 of Baumgartner et al., 1995; De Wever & Caby, 1981; De Wever & Baumgartner, 1995) radiolarians.

The overlying whitish marble (Fig. 6E) is up to tens of metres in thickness, and is made of calcite and ankerite with minor quartz, amphibole, white mica, Fe-oxides and Fe-sulphide. The age of marble is constrained as the Upper Jurassic to Lower Cretaceous (Lemoine et al., 1970), in correlation with the Calpionella Limestone of the non-metamorphosed cover of the Internal Ligurian ophiolites in the Northern Apennines (Principi et al., 2004).

The post-extensional succession continues upward with a 100s of metre–thick calcschist unit, which comprises three discrete members (Fig. 5A). The lower calcschist member (Replatte Formation of Lemoine, 1971) consists of calcite, quartz, white mica and graphite, and its protoliths are made of shale and limestone layers. It locally includes blocks of peridotites, reminiscent of olistoliths *sensu* Festa et al. (2016). This lower calcschist member has been correlated with the

Lower to Upper Cretaceous Palombini Shale overlying the Internal Ligurian ophiolites in the Northern Apennines (Principi et al., 2004).

The middle member (Fig. 5A) is represented by tens of metres thick black micaschist (Roche Noire Formation of Tricart, 1973), which consists mainly of quartz, white mica and graphite. The protolith of this micaschist was fine-grained sandstone with organic material, and its correlates well with the Val Lavagna Schist Group of the Internal Ligurian Units in the Northern Apennines (Lagabrielle, 1994). Black micaschist is transitional upwards into the Gondrand Flysch of Lemoine (1971), which consists of alternating layers of calcschist and metasandstone with clasts of granitoid, metamorphic and carbonate rocks. These clastic rocks are interpreted as Cenomanian and younger deepsea fan deposits, with sediments derived from the European continental margin (Lemoine et al., 1984; Burroni et al., 2003). This uppermost post-extensional sedimentary unit of the QU shows the same stratigraphic position as the Ronco and Canale Formations in the Internal Ligurian Unit ophiolites in the Northern Apennines (Pandolfi & Marroni, 1997; Burroni et al., 2003; Elter et al., 2006).

Chenaillet Ophiolite (CH)

Among the Western Alpine Ophiolites, the CH is the only unit that escaped alpine-stage deformation and metamorphism. Its ophiolite sequence (Figs. 7A and 7B) consists of UM peridotites that were intruded by gabbroic stocks and felsic dykes, and overlain by syn-extensional basaltic lavas and minor sedimentary rocks (Bertrand et al., 1987; Chalot-Pra, 2005; Manatschal et al., 2011). Unlike in the MO and QU, a post-extensional sedimentary sequence does not occur in the CH.

Upper mantle peridotites and mafic and felsic intrusions

Upper mantle units in the CH include serpentinized, spinel-bearing harzburgite and lherzolite (Fig. 8A), with minor plagioclase-bearing lherzolite, dunite, pyroxenite and wherlite (Chalot Pra et al.,

2003). Discontinuous layers of ophicarbonate rocks, up to 10-metres-thick, cover these serpentinized peridotites. Ophicarbonates are made of clasts of peridotites ranging in size from several centimetres to few decimetres in length, and cemented by calcite vein networks (Lafay et al., 2017).

Serpentinized peridotites are intruded by stocks and dykes (tens of metres in width) of troctolite (Fig. 8B) and Mg- and Al-rich gabbro (Fig. 7A). Gabbroic rocks are coarse-grained, contain mainly plagioclase, olivine and clinopyroxene, and show pegmatitic textures. Troctolite and albitite dyke rocks have been dated at 165±1 Ma (Li et al., 2013). Mafic intrusive rocks locally show typical texture of flasergabbro and were deformed along discrete, ductile shear zones, which display high-temperature recrystallization mineral assemblages of augite and hornblende, and veins and pods of leucodiorite as syn-kinematic partial melting products (Mével et al., 1978; Caby, 1995). These leucodiorite veins, which consist of quartz, plagioclase, clinopyroxene and amphibole have been dated at 156±3 Ma (Costa & Caby, 2001). Serpentinite and gabbro units are locally crosscut by Fe- and Ti-rich gabbro dykes, which are composed of clinopyroxene, amphibole, ilmenite and plagioclase (Chalot Pra, 2005; Fig. 7A). Deformed gabbros are also crosscut by 148±2 Ma (Tithonian) albitite dykes (Fig. 8A; Costa & Caby, 2001), indicating a renewed phase of felsic magmatism following the high-temperature ductile deformation and metamorphism. Albitite has also been observed as dykes intrusive into a magmatic breccia consisting of doleritic and basaltic clasts (Chapelle, 1990).

Cataclastic shear zones cap the serpentinite and gabbro units in the CH. Cataclastic gabbro consists of angular clasts of gabbro in a matrix of albite, amphibole, chlorite and epidote. The cataclastically deformed serpentinite represents a matrix-supported serpentine gouge (Fig. 8C). These cataclastic shear zones have been interpreted to represent a detachment fault (Manatschal et al., 2011).

Syn-extensional sedimentary and volcanic sequence

The syn-extensional sedimentary and volcanic sequence in the CH locally starts at the bottom with a 2-metres-thick, matrix- to clast-supported breccia, overlain by graded sandstone and siltstone (Fig. 6). Clasts are irregular to rounded in shape, and are made of serpentinite, gabbro and dolerite (Manatschal et al., 2011). Clastic rocks are overlain by a 400-m-thick volcanic sequence, which is composed of basaltic pillow lava, pillow breccia and hyaloclastite breccia (Fig. 8D). These rocks display MORB geochemical affinities (Chalot Pra, 2005), and are locally interbedded with few decimetres to few metres thick, lensoidal interlayers of sandstone, which is made of pyroxene, spinel and amphibole grains (Bertrand et al., 1984). Sub-volcanic dolerite occurs as both dykes within the underlying serpentinite and gabbro (Fig. 8B), and as hypabyssal bodies and dykes at the bottom and within the volcanic sequence (Chalot Pra, 2005).

Development of the LPO oceanic lithosphere

Our field-based structural and lithostratigraphic observations and the available geochronological data indicate various stages in the evolution of the LPO. We examine this evolutionary trend in four main stages, which may have partially overlapped in time. The first stage was characterized by mafic magmatism and emplacement of gabbroic plutons into the lithospheric mantle. We define this stage as the main magmatic event. Chronological constraints are supported, where possible, by biostratigraphic ages, which are documented to be comparable to radiometric ages (e.g., Bill et al., 2001; Principi et al., 2004; Manatschal et al., 2007 and reference therein).

The second stage was represented by lithospheric-scale extension and detachment faulting, likely aided by thermal weakening related to the emplacement of gabbroic intrusions during the main magmatic event. This episode marks the main tectonic event during the ophiolite formation. The third stage involved renewed magmatism via the eruption of basaltic lava flows and syn-extensional deposition of ophiolitic breccias directly on the previously exhumed, serpentinized peridotites and gabbros. The final stage involved post-extensional deposition of radiolarian chert, limestone, turbiditic sediments and abyssal clay on a rugged seafloor topography within the ocean basin,

shaped by the extensional tectonics. This phase marks a magmatically and tectonically quiet episode in the history of the LPO, prior to its closure. We explain these four stages through a sequential tectonic model (Figs. 9 and 10).

Stage 1: Main magmatic event

Gabbroic bodies in the WAO occur as shallow intrusions, which were emplaced at depths of ~7 to 8 kilometres (Fig. 9A) in the UM peridotites (Chalot Pra et al., 2003; Piccardo et al., 2014) and crystallized in ephemeral magma chambers (Costa & Caby, 2001). These intrusions are composed of troctolite and Mg- and Al-rich gabbros with minor Fe- and Ti-rich gabbros and felsic differentiates. They collectively represent the partial melting products of a lithospheric mantle (Chalot Pra et al., 2003), which was composed of spinel-bearing lherzolite and harzburgite with minor plagioclase-bearing lherzolite (Saccani et al., 2015).

Gabbroic intrusive bodies that are up to several hundreds of metres in thickness occur mainly in the footwalls of detachment faults, which are spatially associated with mylonitic to cataclastic shear zones (Manatschal & Muntener, 2009; Manatschal et al., 2011; Balestro et al., 2015b, 2018; Festa et al., 2015; Lagabrielle et al., 2015). The crystallization ages of these gabbros constrain the timing of their emplacement as the Early to Middle Callovian (165±1 Ma; Li et al, 2013) to Early Oxfordian (163±2 Ma; Rubatto & Hermann, 2003) in the CH and in the MO, respectively. These ages display close temporal relationships with gabbro intrusions in the other WAO ophiolites (165-164 Ma; Rubatto et al., 1998; Rebay et al., 2018). Crystallization ages of similar gabbro intrusions within the UM peridotites in the Northern Apennines ophiolites also range between 165 Ma and 161 Ma (Tribuzio et al., 2016).

Radiometric ages from gabbro intrusions in the QU are lacking but biostratigraphic ages of radiolarian metachert (i.e., Radiolarites *Auct.*) layers, which were deposited on the exhumed upper mantle peridotites and gabbroic intrusions, provide the minimum ages of their emplacement. In the QU, the oldest depositional age of metachert (Middle Bathonian; Cordey & Bailly, 2007) suggests a

pre-Middle Bathonian, likely Bajocian, emplacement age of the oldest gabbro intrusions, if we consider the time span between their crystallization and exhumation from ~7-8 kilometres at depth beneath the seafloor. Taking the base and the top of the Bathonian at 168.3±1.3 Ma and 166.1±1.2 Ma (Cohen et al., 2013), respectively, we can constrain the timing of the emplacement of gabbro intrusions as later than ~167 Ma (middle Bathonian; see also discussion in Cordey & Bailly, 2007). Thus, the emplacement of gabbro intrusions in the WAO peridotites appears to have occurred first in the QU (170-168 Ma), then in the CH (165±1 Ma) and in the MO (163±2 Ma). This interpretation remains valid even when we use different time scales that consider the base and the top of Bathonian at 164.0±2 Ma and 160.0±2 Ma (Odin, 1994) or at 166.0+3.8/-5.6 Ma and 160.4+1.1/-0.5 Ma (Pálfy et al., 2000), respectively. Although more conservatively constrained, a pre-middle Bathonian (likely Bajocian) emplacement age of the oldest gabbro intrusions in the QU is still younger than the gabbro ages documented from the MO (163±2 Ma).

Stage 2: Lithospheric scale extension and upper mantle exhumation

Emplacement of gabbro intrusions into the UM peridotites of the WAO was followed by widespread extensional deformation and the development of lithospheric-scale detachment faults (Fig. 9B; Manatschal et al., 2011; Balestro et al., 2015b; Festa et al., 2015; Lagabrielle et al., 2015). Detachment faulting was accompanied by ductile and brittle deformation episodes, and by the interplay of magmatic, metamorphic, metasomatic and sedimentary processes (see below), which occurred during different stages of UM exhumation. Detachment faulting facilitated progressive uplifting and unroofing of “plum pudding” of discrete gabbro bodies embedded within the host peridotites, as strain localization concentrated along the margins of these gabbro intrusions. This scenario is analogous to those documented from modern, in-situ oceanic core complexes along the slow- (Atlantis Massif, Mid-Atlantic Ridge - MAR) and ultraslow-spreading (Atlantis Bank, Southwest Indian Ridge - SWIR) mid-ocean ridges (e.g., Cannat, 1993; Karson & Lawrence, 1997; Dilek et al.,

1998; Tucholke et al., 1998; Boschi et al., 2006; Dick et al., 2008; MacLeod et al., 2009; Miranda & Dilek, 2010; Escartin et al., 2017).

The high-temperature shear zones observed around the QU and CH gabbros indicate that extensional shearing occurred at the brittle-ductile transition zone at depths of ~8 km (e.g. Manatschal et al., 2011). The associated crystal to plastic deformation developed a mylonitic fabric in the gabbros (i.e., flasergabbro) at temperatures of 700° to 800°C (Mevel et al., 1978). Syn-kinematic partial melting of gabbros at temperatures in excess of 850°C (Caby, 1995) produced leucodioritic veins, dated at 156±3 Ma (Costa and Caby, 2001) in the CH. These observations are similar to those observed at modern and in-situ oceanic core complexes, where high-temperature shear zones evolved into detachment faults in the presence of gabbroic melts (Karson & Dick, 1983; Karson, 1998; MacLeod et al., 2002; Escartin et al., 2008; Miranda & Dilek, 2010; Bonnemains et al., 2017).

Continued extensional deformation and exhumation were accompanied by cooling and metamorphic and metasomatic processes, which produced unique fabrics and mineral assemblages in the host peridotites and their gabbroic intrusions. Up to tens of metres-thick horizons of talcschist and serpentine schist formed along a 20- to 25-kilometres-long shear zone within the MO (i.e., Baracun Shear Zone; see Festa et al., 2015). Shearing and metasomatism were accompanied by amphibolite-facies metamorphism, hydrothermal alteration of gabbros, and production of silica-enriched hydrothermal fluids that interacted with the exhumed ultramafic rocks (Balestro et al., 2015a). These processes collectively caused extensive talc and chlorite schist formation at temperatures ranging between 200°C and 500°C (Bonnemains et al., 2017). Similar occurrences of talc and chlorite schist in narrow shear zones (<100 m), characterized by rock softening and strain localization, have been reported from low-angle detachment faults in the Atlantis Massif core complex along the Mid-Atlantic Ridge (Karson & Lawrence, 1997; Karson et al., 2006; Boschi et al., 2006). Widespread serpentinization of the peridotites was facilitated by downward propagation of fracture networks and played an important role during their exhumation, contributing to the

weakening of the UM rocks, as documented in thermal and rheological models and by their comparison with non-volcanic rifted margin evolution of Western Iberia (Perez-Guissinye & Reston, 2000, and references therein). Penetration of seawater in the UM peridotites of the Lanzo Ultramafic Massif, which represents a well-preserved remnant of mantle rocks in the WAO (Piccardo et al., 2014), has been estimated to reach at least 3 km depth (Debret et al., 2013).

The existence of horizons of ophicarbonate rocks and tectonic breccias along the detachment faults indicates that extensional deformation acquired a brittle mode at shallower depths (~1-3 km) beneath the seafloor both in the MO and CH (Manatschal et al., 2011; Balestro et al., 2015b). In the CH, serpentinite brecciation and carbonate precipitation were polyphase events, which occurred at temperatures ranging between 110°C and 180°C in the presence of long-lived hydrothermal fluid circulations (Lafay et al., 2017). In the MO, exhumation of serpentinized mantle rocks and their gabbroic bodies in the footwall of a detachment fault produced submarine debris flows (i.e., sedimentary breccia), which were then accumulated in wedge-shaped depocentres above this detachment fault that was already exposed on the seafloor (Balestro et al., 2015a). Similar debris flow deposits have been described from the QU, where ophiolitic breccias occur (Tricart & Lemoine, 1983). In the CH, high-angle normal faults, truncating the previously formed low-angle detachment faults (Manatschal et al., 2011) represent the last stage of extensional brittle faulting.

Stage 3: Syn-extensional magmatism and deposition

Serpentinized peridotites, gabbroic plutons, and the detachment surfaces in the WAO were crosscut by doleritic and plagiogranitic dykes and overlain by basaltic pillow and massive lava flows (Fig. 9C). In the CH, basaltic lavas are locally intercalated with hyaloclastites (Chalot Pra, 2005), and volcanic breccias are locally interbedded with ophiolitic sandstones. These relationships provide significant temporal constraints on the timing of detachment faulting and upper mantle exhumation. Plagiogranite intrusions have been constrained in age to 152±2 Ma (i.e., Late Kimmerdigian - Early Tithonian) in the MO (Lombardo et al., 2002). A similar age (148±2 Ma) was obtained from albitite

dykes in the CH (Costa & Caby, 2001). Recent U-Pb zircon dating of gabbro and albitite in the CH (Li et al., 2013) revealed a contemporaneous age of 165±1 Ma for both rocks, suggesting synchronous emplacement of mafic and felsic intrusions during the main magmatic event. However, the occurrence in the CH of albitite dykes crosscutting flasergabbros (Chapelle, 1990) indicates that a younger episode of post–detachment felsic magmatism occurred in this ophiolite. This inference is compatible with the young ages of plagiogranite intrusions in the MO. Furthermore, similar volcanic and intrusive rocks in the Northern Apennine ophiolites have been also dated to the latest Jurassic (i.e., the second magmatic event of Marroni and Pandolfi, 2007). Plagiogranite dykes in the MO have been interpreted as the products of fractional crystallization of evolved magmas (Castelli & Lombardo, 2007; Furnes & Dilek, 2017), which migrated upwards through the exhumed UM peridotites and their gabbroic intrusive bodies during the advanced stages of the seafloor spreading evolution of the LPO (Fig. 9C and 10A).

Radiometric age data from the lavas and felsic intrusions in the QU are lacking. However, the existing biostratigraphic ages of radiolarian metachert of the post-extensional sequence unconformably overlying the metabasalt, meta-ophicarbonates, serpentinized metaperidotites and metagabbros, clearly show that mafic volcanism and felsic dyking in this domain of the LPO must have occurred between Middle Bathonian (~167 Ma) and Late Oxfordian (~158-157 Ma). Syn-extensional magmatism in the QU was temporally associated with the development of detachment faults, and was completed by ~157 Ma. This stage of magmatism and deposition continued into 152±2 Ma in the MO, and possibly until 148±2 Ma in the CH, as constrained by the ages of different generations of felsic dykes described earlier. These age relationships between the pre-alpine magmatic and structural features in the three ophiolite complexes may suggest that the oceanic lithosphere in the QU was already off-axis in the LPO, while detachment faulting, UM exhumation and syn-extensional magmatism were ongoing within the MO and CH along a spreading ridge axis (Fig. 10A).

Basaltic lava flows occupied topographic lows on the exhumed detachment fault surfaces (Chalot Pra et al., 2003; Manatschal et al., 2011) and in the hangingwall units of these detachment faults in the MO and CH (Balestro et al., 2015b; Figs. 9C and 10B). The hyaloclastite deposits locally occurring in the CH may have been produced by gravity flows generated by sub-marine lava flows in the hangingwalls of intraoceanic detachment faults, as documented from slow-spreading ridges and seamounts (Batiza et al., 1984; Smith & Batiza, 1989; Carey & Shneider, 2011, and references therein). Similar spatial relationships between basaltic lavas and detachment faults have been reported from the Atlantis Massif and the MARK area (Mid-Atlantic Ridge by the Kane Fracture Zone; Blackman et al., 1998; Escartin & Canales, 2011). In the MARK area, high–angle normal faults appear to have acted as magma conduits for volcanism, which resulted in the eruption of basaltic lavas directly on the exhumed serpentinized peridotites in their footwalls (Dick et al., 2008).

Stage 4: Post-extensional deposition and tectonic quiescence

The regional unconformity beneath the post-extensional sedimentary sequence (Fig. 9D) marks the temporal boundary between lithospheric-scale extension associated with detachment faulting and UM exhumation and a period of tectonic quiescence during which mainly pelagic deposition took place in and across the LPO (Marroni et al., 2017). A several 100 metres-thick, complete post-extensional metasedimentary sequence (Fig. 9D and 10B) occurs in the QU, covering the exhumed serpentinized metaperidotites with gabbroic meta-intrusive bodies, meta-ophicarbonates, and metabasaltic lavas. The protoliths of metachert, whitish marble, and various calcschist units in this sequence correspond to radiolarite, Calpionella Limestone, and a thick succession of the Palombini Shale and Val Lavagna Group, respectively (see also, e.g., Lemoine et al., 1970; Decandia & Elter, 1972; Lemoine et al., 1984; Lagabrielle, 1994; Burroni et al., 2003). Metachert units invariably occur between ophiolitic metabreccias and pillow metalavas below and a fine-grained pelagic sequence above, and occupy fault controlled structural lows and baythmetric depressions on the palaeo-ocean floor (Fig. 9D and 10B). The overlying whitish marble (stratigraphic

and time equivalent of the Calpionella Limestone), which rests directly on both the serpentinized metaperidotites and the metachert shows variations in thickness from a metre to 10s of metres across the QU. The deposition of the protolith of this marble unit at the Tithonian–Berriasian boundary (i.e., between ~152 and 140 Ma) (Principi et al., 2004, and reference therein) marked the end of active seafloor spreading and the beginning of a tectonically quiet period in the evolutionary history of the LPO (Fig. 10B and 10C). This timing also coincides with widespread deposition of carbonaceous and siliciclastic sediments on the continental margins of both Adria and Europe as well as in the LPO (Principi et al., 2004).

Deposition of the thick, Lower to Upper Cretaceous calcschist succession (i.e., Replatte Formation, Roche Noire Formation and Gondrand Flysch) above the whitish marble continued in the LPO, as thinly bedded marly and calcareous turbidites were mixed with coarse-grained clastic sediments (Fig. 10B), sourced from the European continental margin. These depositional features are identical to those of non-metamorphosed Internal Ligurian Units in the Northern Apennine ophiolites in terms of both their facies (Palombini Shale and Val Lavagna Group) and age (Lower to Upper Cretaceous; Burroni et al., 2003; Elter et al., 2006).

In contrast to the QU, the whitish marble (Calpionella Limestone) at the bottom of the Lower Cretaceous calcschist unit (Palombini Shale) in the post-extensional sequence of the MO is very thin (~several decimetres only). This observation suggests that the post – extensional sequence in the MO may have formed on fault-controlled structural paleo-highs on the seafloor (Figs. 9D and 10B). The lack of any mylonitic or cataclastic structures associated with the uncomformities beneath the whitish marble and the Lower Cretaceous calcschist implies that these contacts correspond to primary depositional surfaces (see Festa et al., 2015 for details). The occurrence of the Lower Cretaceous calcschist resting directly on the upper mantle rocks and syn-extensional sedimentary rocks (see Balestro et al., 2015b; Festa et al., 2015; Figs. 10B and 10C), indicates nearly 7 to 12 million years of non-deposition between the timing of the eruption of syn-etensional basalts (~152±2 Ma) and the deposition of the protolith of this post-extensional calcschist. We, thus, infer, that the

extensional deformation and related upper mantle exhumation along and across the detachment fault were already terminated by the time of the deposition of the Lower Cretaceous calcschist. This time interval of 7–12 m.y. corresponding to the timing of non-deposition coincided with the doming, crustal denudation, syn-extensional clastic deposition, and exhumation of an oceanic core complex in the MO domain of the LPO (Fig. 10C).

Modern oceanic core complexes along the MAR form dome-shaped bathymetric highs (up to 3000 metres) above the seafloor, and display striated and corrugated megamullion surfaces (detachment faults) that extend for several tens of kilometres (10 to 40 km) across and over hundreds of square kilometres in area (Escartin et al., 2017, and references therein). Some of these corrugated detachment surfaces are shown to have accommodated down-dip slips at a rate of 125 millimetres per year (Yu et al. 2013; Fruh-Green et al. 2017). Syn-extensional basaltic lavas and deposits resting on these modern oceanic core complexes along the MAR and SWIR represent supradetachment basin products (Blackman et al. 1998; Karson et al., 2006; Escartin & Canales 2011; Hayman et al., 2011), analogous to their counterparts in continental core complexes (Oner & Dilek 2013).

Conclusions

The results of this study show that the development of the pre-alpine structure and stratigraphy of the WAO and the evolution of the LPO involved seafloor spreading of a restricted ocean basin between Europe and Adria in a ~25 to 30 million years of time interval from the Middle Jurassic (~170-168 Ma) to the Late Jurassic–Early Cretaceous. This seafloor spreading evolution of the LPO took place in four main stages that are well defined by tectonic, magmatic and depositional features in the rock record of the WAO. Emplacement of gabbro bodies in the upper mantle peridotites occurred in the pre-middle Bathonian (i.e. <167 Ma), middle Callovian (i.e., 165±1), and late Callovian–early Oxfordian (163±2 Ma) in the QU, CH and MO, respectively, and marked Stage 1. Widespread extensional deformation characterized by lithospheric–scale detachment faulting,

upper mantle exhumation–denudation, and doming marked Stage 2 in the evolution of the LPO. This extensional deformation was initially aided by thermal weakening associated with the emplacement of gabbro intrusions. These processes were analogous to to those documented from modern slow- (Atlantis Massif, MAR) and ultraslow-spreading (Atlantis Bank, SWIR) ridges (Karson and Lawrence, 1997; Cannat et al., 2006; Karson et al., 2006; Ildefonse et al., 2007; Miranda & Dilek, 2010). Emplacement of basaltic dykes into the exhumed peridotites and gabbroic plutons, and eruption of basaltic lavas on these mafic and ultramafic basement rocks occurred during a period of syn-extensional magmatism, marking Stage 3. This stage also involved the deposition of ophiolitic breccias. Serpentinized peridotites with their gabbroic intrusions and the syn–extensional volcanic and sedimentary sequences in the WAO were subsequently overlain by pelagic sediments (now represented by metachert, white marble and calcschist) during Stage 4, when a tectonic quiescence period prevailed within the LPO.

The WAO display significant structural and magmatic evidence for the seafloor spreading evolution of the LPO despite the multi–phase, subduction– and collision–induced deformational and metamorphic overprint. Biostratigraphic and geochronological data in different ophiolite complexes in the WAO reflect a snapshot view of diachronous development of a slow–spread oceanic lithosphere in different domains within a restricted ocean basin. The mode and tempo of the documented tectonic, magmatic and depositional processes that shaped the internal structure of the WAO are significantly different from those described from modern and ancient suprasubduction zone oceanic lithosphere types. Thus, the structural architecture and the evolutional history of the WAO may potentially serve as a template for those subduction–unrelated ophiolites, derived from downgoing lower oceanic plates during the closure of small ocean basins.

Acknowledgements

We extend our sincere thanks to Drs A. Borghi, D. Castelli, G. Fioraso, C. Groppo, M. Gattiglio and P. Tartarotti for discussions on the geology of the Western Alps. We thank Associate Editor T.O.

Rooney for his constructive comments on the manuscript, and J.A. Karson, H. Furnes and an anonymous referee for their critical and thorough reviews, from which we have benefited greatly in revising our manuscript. We are grateful to S. Cavagna for sample preparation. This study has been supported by 'Ricerca Locale (ex 60%) 2014, 2015, 2016, 2017, 2018' of the Università degli Studi di Torino (grants to A. Festa), the Italian Ministry of University and Research (PRIN 2010/2011: grants n. 2010AZR98L_002 to A. Festa; PRIN 2015: grants n. 2015EC9PJ5 to G. Balestro), and the Italian Ministry of University and Research ("Finanziamento annuale individuale delle attività base di ricerca" 2017) to G. Balestro and A. Festa. Y. Dilek acknowledges the Miami University Distinguished Professor discretionary funds in support of his fieldwork in the Western Alps.

References

Angiboust, S., Langdon, R., Agard, P., Waters, D. & Chopin, C. 2012. Eclogitization of the Monviso ophiolite (W. Alps) and implications on subduction dynamics. *Journal of Metamorphic Geology,* **30**, 37–61.

Argand, E. 1911. Sur la repartition des roches vertes mésozoïques dans les Alpes Pennines avant la formation des grands plis couches. *Bulletin de la Societé Vaudoise de Sceiences Naturelles*, **47**, 1-2.

Batiza, R, Fornari, D.J., Vanko, D., & Lonsdale, P. 1984. Craters, calderas and hyaloclastites: common features if young Pacific seamounts. *Journal of Gephysical Research,* **89**, 8371-8390.

Balestro, G., Cadoppi, P., Perrone, G. & Tallone, S. 2009. Tectonic evolution along the Col del Lis-Trana Deformation Zone (internal Western Alps). *Italian Journal of Geosciences*, **128**(2), 331-339, doi: 10.3301/IJG.2009.128.2.331

Balestro, G., Festa, A. & Tartarotti, P. 2015a. Tectonic significance of different block-in matrix structures in exhumed converget plate margins: examples from oceanic and continental HP rocks in Inner Western Alps (northwest Italy). *International Geology Review,* **57** (5–8), 581–605.

Balestro, G., Festa, A., Dilek, Y. & Tartarotti, P. 2015b. Pre-Alpine extensional tectonics of a peridotite-localized oceanic core complex in the late Jurassic, high-pressure Monviso ophiolite (Western Alps). *Episodes,* **38** (4), 266–282, doi:10.18814/epiiugs/2015/v38i4/82421

Balestro, G, Festa, A., Borghi, A., Castelli, D., Gattiglio, M. & Tartarotti P. 2018. Role of Late Jurassic intra-oceanic structural inheritance in the Alpine tectonic evolution of the Monviso meta-ophiolite Complex (Western Alps). *Geological Magazine*, **155**(2), 233-249.Balestro, G., Fioraso, G. & Lombardo, B. 2011. Geological map of the upper Pellice Valley (Italian Western Alps). *Journal of Maps*, **2011**, 634-654. doi: 10.4113/jom.2011.1213.

Balestro, G., Fioraso, G. & Lombardo, B. 2011. Geological map of the upper Pellice Valley (Italian Western Alps). *Journal of Maps*, **2011**, 634-654. doi: 10.4113/jom.2011.1213.

Balestro, G., Fioraso, G. & Lombardo, B. 2013. Geological map of the Monviso massif (Western Alps). *Journal of Maps,* **9** (4), 623-634. doi: 10.1080/17445647.2013.842507.

Balestro, G., Lombardo, B., Vaggelli, G., Borghi, A., Festa, A. & Gattiglio, M. 2014. Tectonostratigraphy of the northern Monviso meta-ophiolite complex (Western Alps). *Italian Journal of Geosciences,* **133** (3), 409–426, doi:10.3301/IJG.2014.13

Ballèvre M., Lagabrielle Y. & Merle O. 1990. Tertiary ductile normal faulting as a consequence of lithospheric stacking in the western Alps. *Mémoire Societé géologique de France,* **156**, 227-236.

Ballèvre, M. & Merle, O. 1993. The Combin Fault: compressional reactivation of a Late Cretaceous–Early Tertiary detachment fault in the western Alps. *Schweizerische Mineralogische und Petrographische Mitteilungen*, **73**, 205–227.

Baumgartner, P.O., Bartolini, A., Carter, E.S., Conti, M., Cortese, G., Danelian, T., De Wever, P., Dumitrica, P., Dumitrica-Jud, R., Gorican, S., Guex, J., Hull, D.M., Kito, N., Marcucci, M., Matsuoka, A., Murchey, B., O'Dogherty, L., Savary, J., Vishnevskaya, V., Widz, D. & Yao, A. 1995. Middle Jurassic to Early Cretaceous radiolarian biochronology of Tethys based on unitary associations. *In* Baumgartner, P.O., et al. (Eds.), Middle Jurassic to Lower Cretaceous Radiolaria of Tethys: Occurrences, systematics, biochronology. *Mémories Géologie*, Lausanne, **23**, 1013-1043.

Bearth, P. 1967. Die Ophiolithe der Zone von Zermatt-Saas Fee. *Beiträge zur Geologischen Karte der Schweiz, Neue Folge,* **132**, 1-130.

Bernouilli, D., Manatschal, G., Desmurs, L. and Müntener, O. 2003. Where did Gustav Steinmann see the trinity? Back to the roots of an Alpine ophiolite concept. In, Dilek Y. & Newcomb, S. (eds.), Ophiolite concept and the evolution of the geological though, Boulder, CO, *Geological Society of America Special Paper*, **373**, 93-110.

Bertrand, J., Dietrich, V., Nievergelt, P. & Vuagnat, M. 1987. Comparative major and trace element geochemistry of gabbroic and volcanic rock sequences, Montgenèvre ophiolite, Western Alps. *Schweizerische Mineralogische und Petrographische Mitteilungen*, **67**, 147–169.

Bertrand, J., Nievergelt, P. & Vuagnat, M. 1984. Oceanic sedimentary processes and alpine metamorphic events in the Montgenevre ophiolite, Western Alps. *Ofioliti*, **9**(3), 303-320.

Bill, M., O'Dogherty, L., Guex, J., Baumgartner, P. O. & Masson, H. 2001. Radiolarite ages in Alpine-Mediterranean ophiolites: Constraints on the oceanic spreading and the Tethys–Atlantic connection. *Geological Society of America Bulletin*, **113**, 129–143.

Blackman, D.K., Cann, J.R., Janssen, B. & Smith, D.K. 1998. Origin of extensional core complexes: Evidence from the Mid-Atlantic Ridge at Atlantis Fracture Zone. *Journal of Geophysical Research*, **103**, 21315–21333, doi:10.1029/98JB01756.

Bogatto S. & Castelli D. 1997. Primary and coronitic to metasomatic mineral assemblages in rodingitic Mg-, Cr- and Fe-Tigabbros from the Monviso ophiolite (Val Varaita, italian Western Alps). *Quaderni di Geodinamica Alpina e Quaternaria*, **4**, 160-161.

Bonnemains D., Escartin J., Mevel C, Andreani M. & Verlaguet A. 2017. Pervasive silicification and hanging wall overplating along the 13°20'N oceanic detachment fault (Mid-Atlantic Ridge). *Geochemistry Geophysics Geosystems*, **18**(6), 2028-2053.

Boschi, C., Früh-Green, G.L. & Delacour, A. 2006. Mass transfer and fluid flow during detachment faulting and development of an oceanic core complex, Atlantis Massif (MAR 30°N). *Geochemistry, Gephysics, Geosystems* **7**, doi:10.1029/2005GC001074.

Brogniart, A. 1921. Sur le gisement ou position relative des ophiolites, euphotides, jaspes, etc. dans quelques parties des Apennins. *Annales des Mines ou recueuil de Mémoires sur l'Exploitation des Mines*, **6**, 177-238.

Burroni, A., Levi, N., Marroni, M. & Pandolfi, L. 2003. Lithostratigraphy and structure of the Lago nero Unit (Chenaillet Massif, Western Alps): comparison with Internal Liguride Units of Northern Apennines. *Ofioliti*, **28**(1), 1-11.

Butler, J.P., Beaumont, C. & Jamieson, R.A. 2013. The Alps 1: A working geodynamic model for burial and exhumation of (ultra)high-pressure rocks in Alpine-type orogens. *Earth and Planetary Science Letters*, **377–378**, 114–131, doi:10.1016/j.epsl.2013.06.039

Caby, R., 1995. Plastic deformation of gabbros in a slow-spreading Mesozoic Ridge: example of the Montgenèvre Ophiolite. In: Vissers, R.L.M., Nicolas, A. (Eds.) *Mantle and Lower Crust Exposed in Oceanic Ridges and in Ophiolites,* Kluwer Academic Publishers, 123–145.

Cannat, M. 1993. Emplacement of mantle rocks in the seafloor at Mid-Ocean ridge. *Journal of Geophysical Research,* **98**, 4163-4172.

Cannat, M., Sauter, D., Mendel, V., Ruellan, E., Okino, K., Escartin, J., Combier, V. & Baala, M. 2006. Modes of seafloor generation at a melt-poor ultraslow-spreading ridge. *Geology*, **34**, 605-608, doi:10.1130/G22486.1

Capponi, G., Festa, A., and Rebay, G., 2018, Birth and death of oceanic basins: geodynamic processes from rifting to continental collision in Mediterranean and circum-Mediterranean orogens. *Geological Magazine*, **155** (2), 233-249. Doi: 10.1017/S0016756817001066

Carey, S.N. & Schneider, J-L. 2011. Deep-Sea sediments. *Development in Sedimentology,* **63**, 457-515.

Carpéna, J. & Caby, R. 1984. Fission-track evidence for late Triassic oceanic crust in the French Occidental Alps. *Geology*, **12**, 108-111.

Castelli, D. & Lombardo, B. 2007. The plagiogranite – FeTi-oxide gabbro association of Verné (Monviso metamorphic ophiolite, western Alps). *Ofioliti* **32**, 1-14.

Chalot-Prat, F. 2005. An undeformed ophiolite in the Alps: field and geochemical evidence for a link between volcanism and shallow plate tectonic processes. In Foulger, G.R., Natland, J.H., Presnall, D.C., Anderson, D.L. (Eds.) *Plates, Plumes and Paradigms*. Geological Society of America Special Papers, **388**, 751–780.

Chalot-Prat, F., Ganne, J. & Lombard, A. 2003. No significant element transfer from the oceanic plate to the mantle wedge during subduction and exhumation of the Tethys Ocean (western Alps). *Lithos*, **69**, 69–103, doi: 10.1016/S0024-4937(03)00047-1.

Chapelle, B. 1990. La lithosphère océanique de la Téthys ligure. Etude des magmatismes basiques et acides (massifs ophiolitiques du Montgenèvre et de Haute-Ubaye). PhD Thesis, Grenoble, France, 196 pp.

Cohen, K.M., Finney, S.C., Gibbard, P.L. & Fan, J.-X., 2013 (updated 2018/08). The ICS International Chronostratigraphic Chart. *Episodes*, **36**, 199-204.

Compagnoni, R., Rolfo, F. & Castelli, D. 2012. Jadeitite from the Monviso meta-ophiolite, western Alps: occurrence and genesis. *European Journal of Mineralogy,* **24**, 333-343.

Cordey, F. & Bailly, A. 2007. Alpine ocean seafloor spreading and onset of pelagic sedimentation: New radiolarian data from the Chenaillet-Montgenevre ophiolite (French-Italian Alps). *Geodinamica Acta*, **20**, 131–138.

Costa, S. & Caby, R., 2001. Evolution of the Ligurian Tethys in the Western Alps: Sm/Nd and U/Pb geochronology and rare-earth element geochemistry of the Montgenève ophiolite (France). *Chemical Geology*, **175**, 449–466.

Coward, M.P. & Dietrich, D. 1989. Alpine tectonics-an overview. *In* Coward, M.P., Dietrich, D. & Park, R.G. (Eds) *Alpine tectonics*, Geological Society, London, Special Publications, **45,** 1-29**,** doi:10.1144/GSL.SP.1989.045.01.01

Clari, P.A., Dela Pierre, F., & Martire, L. 1995. Discontinuities in carbonate successions: identification, interpretation and classification of some Italian examples. *Sedimentary Geology,* **100**, 97-121.

Dal Piaz, G.V., Bistacchi, A. & Massironi, M. 2003. Geological outline of the Alps. *Episodes,* **26**, 175–180.

Dal Piaz, G.V., Hunziker, J.C. & Martinotti G. 1972. La Zona Sesia-Lanzo e l'evoluzione tettoni-co-metamorfica delle Alpi nordoccidentali interne. *Memorie Società Geologica Italiana*, **11**, 433-466.

Decandia, FA & Elter, P. 1972. La zona ofiolitifera del Bracco nel settore compreso tra Levanto e la Val Graveglia (Appennino Ligure). *Memorie Società Geologica Italiana*, **11**, 503–530.

Deville E., Fudral S., Lagabrielle Y., Marthaler M. & Sartori M. 1992. From oceanic closure to continental collision: A synthesis of the "Schistes lustrés" metamorphic complex of the Western Alps. *Geological Society of America Bulletin*, **104**, 127-139.

De Wever, P. & Baumgartner, P. O. 1995. Radiolarians from the base of the supra-ophiolitic Schistes Lustrés Formation in the Alps (Saint-Véran, France and Traversiera Massif, Italy). In Baumgartner, P.O. et al. (Eds.), *Middle Jurassic to Lower Cretaceous Radiolaria of Tethys: Occurrences, systematics, biochronology.* Lausanne Mémoires de Géologie, **23**, 725–730.

De Wever, P. & Caby, R. 1981. Datation de la base des Schistes lustrés postophiolitiques par des radiolaires (Oxfordien supérieur-Kimméridgien moyen) dans les Alpes Cottiennes (Saint-Véran, France). *Comptes Rendus de l'Académie des Sciences Paris*, **292**, 467–472.

De Wever, P., Danelian, T., Durand-Delga, M., Cordey, F. & Kito, N. 1987. Datations des radiolarites post-ophiolitiques de Corse alpine à l'aide des Radiolaires. *Comptes Rendus de l'Académie des Sciences Paris*, **305**, 893–900.

Debret., B, Nicollet, C., Andreani, M., Schwartz, S & Godard, M. 2013. Three steps of serpentinization in an eclogitized oceanic serpentinization front (Lanzo Massif – Western Alps). *Journal of Metamorphic Geology*, **31**, 165-168.

Dick, H.J.B. & Mével, C. 1996. The Ocean Lithosphere and Scientific Drilling into the 21st Century. JOI/U.S. Science Support Program and InterRidge, Washington, D.C., 89 pp.

Dick, H.J.B., Tivey, M.A. & Tucholke, B.E. 2008. Plutonic foundation of a slow-spreading ridge segment: Oceanic core complex at Kane Megamullion, 2330′N, 4520′W. *Geochemistry, Geophysics, Geosystems*, **9**, Q05014, doi:10.1029/2007GC001645.

Dilek, Y. 2003. Ophiolite concept and its evolution. In, Dilek Y. & Newcomb, S. (eds.) Ophiolite concept and the evolution of geological thought, *Geological Society of America Special Paper*, **373**, 1-16.

Dilek, Y. 2006. Collision tectonics of the Eastern Mediterranean region: Causes and consequences. *Geological Society of America Special Paper* **409**, 1-13. DOI: 10.1130/2006.2409(1).

Dilek, Y. & Eddy, C.A. 1992. The Troodos (Cyprus) and Kizildag (S. Turkey) ophiolites as structural models for slow-spreading ridge segments. *Journal of Geology*, **100**, 305-322.

Dilek, Y. & Flower, M.F.J. 2003. Arc-trench rollback and forearc accretion: 2. Model template for Albania, Cyprus and Oman: In, Dilek Y. & Robinson, P.T. (Editors), Ophiolites in Earth History, Geological Society of London Special Publication **218**, p. 43-68.

Dilek, Y. & Robinson, P.T. 2003. Ophiolites in Earth History: Introduction. In, Dilek Y & Robinson, P.T. (Editors), *Ophiolites in Earth History, Geological Society of London Special Publication* **218**, 1-8.

Dilek, Y. & Furnes, H. 2009. Structure and geochemistry of Tethyan ophiolites and their petrogenesis in subduction rollback systems. *Lithos*, **113**, 1-20. DOI: 10.1016/j.lithos.2009.04.022.

Dilek, Y & Furnes, H. 2011. Ophiolite genesis and global tectonics: Geochemical and tectonic fingerprinting of ancient oceanic lithosphere. *The Geological Society of America Bulletin* **123**, 387-411, DOI: 10.1130/B30446.1

Dilek, Y., & Furnes, Y. 2014. Origins of ophiolites. *Elements* **10**, 93-100. DOI: 10.2013/gselements.10.2.93

Dilek, Y., & Thy, P. 2009. Island arc tholeiite to boninitic melt evolution of the Cretaceous Kizildag (Turkey) ophiolite: Model for multi-stage early arc-forearc magmatism in Tethyan subduction factories. *Lithos*, **113**, 68-87, DOI: 10.1016/j.lithos.2009.05.044.

Dilek, Y., Thy, P., Moores, E.M. & Ramsden, T.W. 1990. Tectonic evolution of the Troodos ophiolite within the Tethyan framework. *Tectonics*, **9**, 811-823. DOI: 10.1029/TC009i004p00811.

Dilek, Y., Moores, E.M. & Furnes, H. 1998. Structure of modern oceanic crust and ophiolites and implications for faulting and magmatism at oceanic spreading centers. In R. Buck, J. Karson, P. Delaney and Y. Lagabrielle (Editors), American Geophysical Union Monograph on Faulting and Magmatism at Mid-Ocean Ridges, **106**, 219-266.

Dilek, Y., Furnes, H. & Shallo, M. 2007. Suprasubduction zone ophiolite formation along the periphery of Mesozoic Gondwana. *Gondwana Research* **11**, 453-475. DOI: 10.1016/j.gr.2007.01.005

Elter, G. 1971. Schistes lustrés et ophiolites de la zone piemontaise entre Orco et Doire Baltée (Alpes Graies). Hypotèses sur l'origine des ophiolites. *Gèologie Alpine*, **47**, 147-169.

Elter, P., Lasagna, S., Marroni, M., Pandolfi, L., Vescovi, P. & Zanzucchi, G. 2006. Foglio 215 Bedonia della Carta Geologica d'Italia in scala 1:50.000 e note illustrative. Istituto Poligrafico e Zecca dello Stato, Roma.

Escartin, J. & Canales, J.P. 2011. Detachments in oceanic lithosphere: Deformation, magmatism, fluid flow and ecosystems. *Eos Transactions American Geophysical Union*, **92**, 31, http://dx.doi.org/10.1029/2011EO040003

Escartín, J., Mével, C., MacLeod, C.J. & McCaig, A.M. 2003. Constraints on deformation conditions and the origin of oceanic detachments: The Mid-Atlantic Ridge core complex at 15°45′N. *Geochemistry Geophysics Geosystems*, **4(8)**, 1-37, doi:10.1029/2002GC000472

Escartìn, J., Smith, D.K., Cann, J., Schouten, H., Langmuir, C.H. & Escrig, S. 2008. Central role of detachment faults in accretion of slowspread oceanic lithosphere. *Nature*, **455**, 790–794.

Escartín, J., Mével, C., Petersen, S., Bonnemains, D., Cannat, M., Andreani, M., Augustin, N., Bezos, A., Chavagnac, V., Choi, Y., Godard, M., Haaga, K., Hamelin, C., Ildefonse, B., Jamieson, J., John, B., Leleu, T., MacLeod, C.J., Massot-Campos, M., Nomikou, P., Olive, J.A., Paquet, M., Rommevaux, C., Rothenbeck, M., Steinfuhrer, A., Tominaga, M., Triebe, L., Campos, R., Gracias, N. & Garcia, R. 2017. Tectonic structure, evolution, and the nature of oceanic core complexes and their detachment fault zones (13°20′N and 13°30′N, Mid Atlantic Ridge). *Geochemistry Geophysics Geosystems*, **18**, 1451-1482

Festa, A., Balestro, G., Borghi, A., De Caroli S. & Succo, A. 2019. The role of structural inheritance in continental break-up and exhumation of Alpine Tethyan mantle (Canavese Zone, Western Alps). *Geoscience Frontiers*, https://doi.org/10.1016/j.gsf.2018.11.007

Festa, A., Balestro, G., Dilek, Y. & Tartarotti, P. 2015. A Jurassic oceanic core complex in the high-pressure Monviso ophiolite (western Alps, NW Italy). *Lithosphere,* **7**, 646–652, doi:10.1130/L458.1

Festa, A., Ogata, K., Pini, G.A., Dilek, Y. & Alonso, J.L. 2016. Origin and significance of olistostromes in the evolution of orogenic belts: A global synthesis. *Gondwana Research*, **39**, 180-203. Doi: http://dx.doi.org/10.1016/j.gr.2016.08.002

Froitzheim, N., and G. Manatschal, G. 1996. Kinematics of Jurassic rifting, mantle exhumation, and passive-margin formation in the Austroalpine and Penninic nappes (eastern Switzerland). *Geological Society of America Bulletin*, **108**, 1120-1133.

Früh-Green, G.L., Orcutt, B.N., Green, S.L., Cotterill, C., Morgan, S., Akizawa, N., Bayrakci, G., Behrmann, J.-H., Boschi, C., Brazleton, W.J., Cannat, M., Dunkel, K.G., Escartin, J., Harris, M., Herrero-Bervera, E., Hesse, K., John, B.E., Lang, S.Q., Lilley, M.D., Liu, H.-Q., Mayhew, L.E., McCaig, A.M., Menez, B., Morono, Y., Quéméneur, M., Rouméjon, S., Sandaruwan Ratnayake, A., Schrenk, M.O., Schwarzenbach, E.M., Twing, K.I., Weis, D., Whattham, S.A., Williams, M., and Zhao, R., 2017. Expedition 357 summary. In Früh-Green, G.L., Orcutt, B.N., Green, S.L., Cotterill, C., and the Expedition 357 Scientists (Eds.), *Atlantis Massif Serpentinization and Life*, proceedings of the International Ocean Discovery Program, **357**, doi:10.14379/iodp.proc.357.101.2017

Furnes, H. & Dilek, Y., 2017. Geochemical characterization and petrogenesis of intermediate to silicic rocks in ophiolites: A global synthesis. *Earth-Science Reviews*, **166**, 1-37.

Giacometti, F., Evans, K.A., Rebay, G., Cliff, J., Tomkins, A., Rossetti, P., Vaggelli, G. & Adams, D. 2014. Sulfur isotope evolution in sulfide ores from Western Alps: assessing the influence of

subduction-related metamorphism. *Geochemistry Geophysics Geosystems*, **15**(10), 3808-3829.

Goodenough, K.M, Thomas, B., Styles, M., Schofield, D.I. & McLeod, C.J. Records of Ocean Growth and Destruction in the Oman-UAE Ophiolite. *Elements*, **10**, 105-110. DOI: 10.2113/gselements.10.2.109.

Groppo, C. & Castelli, D. 2010. Prograde P–T evolution of a lawsonite eclogite from the Monviso Meta-ophiolite (Western Alps): Dehydration and redox reactions during subduction of oceanic FeTi-oxide gabbro. *Journal of Petrology,* **51**, 2489–2514, doi:10.1093/petrology/egq065

Handy, M.R., Schmid, S.M., Bousquet, R., Kissling, E. & Bernoulli, D. 2010. Reconciling plate-tectonic reconstructions of Alpine Tethys with the geological-geophysical record of spreading and subduction in the Alps. *Earth Science Reviews*, **102**, 121-158.

Hayman, N.W., Grindlay, N.R., Perfit, M.R., Mann, P., Leroy, S. & de Lépinay, B.M. 2011. Oceanic core complex development at the ultraslow spreading Mid-Cayman Spreading Center. *Geochemistry Geophysics Geosystems*, **12**(3), doi: 10.1029/2010GC003240.

Ildefonse, B., Blackman, D.K., John, B.E., Ohara, Y., Miller, D.J. & MacLeod, C.J. 2007. Oceanic core complexes and crustal accretion at slow-spreading ridges. *Geology*, **35**, 623–626, https://doi:10.1130/G23531A.1

Karson, J. A. 1998. Internal structure of oceanic lithosphere: A perspective from tectonic windows, in Faulting and Magmatism at Mid-ocean Ridges. *Geophysical Monograph Series*, **106**, 177–218.

Karson, J.A. & Dick, H.J.B. 1983. Tectonics of ridge-transform intersections at the Kane Fracture Zone, 24°N on the Mid-Atlantic Ridge. *Marine Geophysical Researches*, **6**, 51-98.

Karson, J.A. & Lawrence, R.M. 1997. Tectonic setting of serpentinite exposures on the western median valley wall of the MARK Area in the vicinity of Site 920. *In* Karson, J.A., Cannat, M., Miller, D.J. & Elthon D. (Eds), Proceedings of the Ocean Drilling Program, Scientific Results, **153**, 5-22.

Karson, J.A., Früh-Green, G.L., Kelley, D.S., Williams, E.A., Yoerger, D.R. & Jakuba, M. 2006. Detachment shear zone of the Atlantis Massif core complex, Mid-Atlantic Ridge, 30° N. *Geochemistry Geophysics Geosystems*, **7**(6), Q06016, doi:10.1029/2005GC001109.

Kerckhove, C., Gidon, M., Malaroda, R., Barfety, J. C., Bogdanoff, S. & Lemoine, M. 1979. Carte géologique de la France à 1:250 000, feuille 35 Gap, BRGM, Orléans.

Lafay R., Baumgartner Lukas., Schwartz S., Picazo S., Montes-Hernandez G. & Vennemann T. 2017. Petrologic and stable isotopic studies of a fossil hydrothermal system in ultramafic environment (Chenaillet ophicalcites, Western Alps, France): processes of carbonate cementation. *Lithos*, **294-295**, 319-338.

Lafay, R., Deschamps, F., Schwartz, S., Guillot, S., Godard, M., Debret, B. & Nicollet, C. 2013. High-pressure serpentinites, a trap-and-release system controlled by metamorphic conditions: Example from the Piedmont zone of the western Alps. *Chemical Geology*, **343**, 38–54, doi:10.1016/j.chemgeo.2013.02.008

Lagabrielle, Y., 1987. Les ophiolites: marqueurs de l'histoire tectonique des domains océaniques, unpublished thesis. Brest 350 p.

Lagabrielle Y. 1994. Ophiolites of the Western Alps and the nature of the Tethyan oceanic lithosphere. *Ofioliti*, **19**, 413-434.

Lagabrielle, Y. & Polino, R., 1985. Origine volcano-détritique de certaines prasinites des Schistes lustrés du Queyras (France): arguments texturaux et géochimiques. *Bulletin de la Société géologique de France*, **4**, 461-471.

Lagabrielle, Y. & Polino, R. 1988. Un schéma structural du domaine des Schistes lustrés ophiolitifères au nord-ouest du massif du Mont Viso (Alpes sud-occidentales) et ses implications. *Comptes rendus de l'Académie des Sciences*, **306** (II), 921-928.

Lagabrielle Y., Vitale Brovarone A. & Ildefonse B. 2015. Fossil oceanic core complexes recognized in the blueschist metaophiolites of Western Alps and Corsica. *Earth-Science Reviews*, **141**, 1-26.

Lavier, L. & Manatschal, G. 2006. A mechanism to thin the continental lithosphere at magma-poor margins. *Nature*, **440**, 324-328, doi: 10.1038/nature04608.

Laubscher, H.P. 1991. The arc of Western Alps today. *Eclogae Geologicae Helvetiae*, **84**, 631–659.

Lemoine, M. 1971. Données nouvelles sur la série du Gondran près Briançon (Alpes Cottiennes). Réflexions sur les problèmes stratigraphique et paléogéographique de la zone piémontaise. *Géologie Alpine*, **47**, 181-201.

Lemoine M. & Tricart P. 1986. Les Schistes lustrés piémontais des Alpes Occidentales: Approche stratigraphique, structural et sédimentologique. *Eclogae Geologicae Helvetiae*, **79**, 271-294.

Lemoine, M., Tricart, P. & Boillot, G. 1987. Ultramafic and gabbroic ocean floor of the Ligurian Tethys (Alps, Corsica, Apennines): in search of a genetic model. *Geology*, **15**, 622-625.

Lemoine. M.. Marthaler. M., Caron, M., Sartori. M.. Amaudric Du Chaffaut, S., Dumont, T., Escher, A., Masson, H., Polino, R. & Tricart, P. 1984. Découverte de foraminifères planctoniques du Crétacé supérieur dans les Schistes lustrés du Queyras (Alpes occidentales): conséquences paléogéographiques et tectoniques. *Comptes Rendus Acadmie Science Paris*, **11**,727-731.

Li, X., Faure, M., Lin, W. & Manatschal, G. 2013. New isotopic constraints on age and magma genesis of an embryonic oceanic crust: The Chenaillet Ophiolite in the Western Alps. *Lithos*, **160-161**, 283-291.

Lemoine, M., Steen, D. & Vuagnat, M. 1970. Sur le problème des ophiolites piémontaises et des roches sédimentaires associées : observations dans le massif de Chabrière en Haute-Ubaye. *Comptes Rendus des Séances*, **5**(1), 44-59.

Lombardo, B. & Pognante, U. 1982. Tectonic implications in the evolution of the Western Alps ophiolite metagabbros. *Ofioliti*, **7**, 371-394.

Lombardo, B., Rubatto, D. & Castelli, D. 2002. Ion microprobe U–Pb dating of zircon from a Monviso metaplagiogranite: Implications for the evolution of the Piedmont-Liguria Tethys in the Western Alps. *Ofioliti,* **27**, 109–117.

Lombardo, B., Nervo, R., Compagnoni, R., Messiga, B., Kienast, J., Mevel, C., Fiora, L., Piccardo, G. & Lanza, R. 1978. Osservazioni preliminari sulle ofioliti metamorfiche del Monviso (Alpi Occidentali). *Rendiconti Società Italiana di Mineralogia e Petrologia,* **34**, 253–305.

MacLeod, C.J., Escartin; J., Banerji, D., Banks, G.J., Gleeson, M., Irving, D.H.B., Lilly, R.M., McCaig, A.M., Niu, Y, Allerton,S. & Smith, D.K. 2002. Direct geological evidence for oceanic detachment faulting: The Mid-Atlantic Ridge, 15°45'N. *Geology*, **30**, 879-882.

MacLeod, C.J., Searle, R.C., Murton, B.J., Casey, J.F., Mallows, C., Unsworth, S.C., Achenbach, K. L. & Harris, M. 2009. Life cycle of oceanic core complexes. *Earth and Planetary Science Letters*, **287**(3-4), 333-344.

Manatschal, G. 2004. New models for evolution of magma-poor rifted margins based on a review of data and concepts from West Iberia and the Alps. *International Journal of Earth Sciences*, **93**, 432-466, doi:10.1007/s00531-004-0394-7.

Manatschal, G. & Bernoulli, D. 1999. Architecture and tectonic evolution of nonvolcanic margins: Present day Galicia and ancient Adria. *Tectonics*, **18**, 1099–1119

Manatschal, M. & Müntener, O. 2009. A type sequence across an ancient magma-poor ocean–continent transition: the example of the western Alpine Tethys ophiolites. *Tectonophysics*, **473**, 4–19.

Manatschal, G., Müntener, O., Lavier, L.L., Minshull, T.A., Péron-Pinvidic, G., 2007. Observations from the Alpine Tethys and Iberia–Newfoundland margins pertinent to the interpretation of continental breakup. In: Karner, G.D., Manatschal, G., Pinheiro, L.M. (Eds.), Imaging, mapping and modelling continental lithosphere extension and breakup. Geological Society of London, Special Publications, vol. 187, pp. 291–324.

Manatschal, G., Sauter, D., Karpoff, A.M., Masini, E., Mohn, G. & Lagabrielle, Y. 2011. The Chenaillet Ophiolite in the French/Italian Alps: an ancient analogue for an Oceanic Core Complex? *Lithos,* **124**, 169–184.

Marroni, M. & Pandolfi, L. 2007. The architecture of an incipient oceanic basin: a tentative reconstruction of the Jurassic Liguria–Piemonte basin along the Northern Apennines–Alpine Corsica transect. *International Journal of Earth Sciences*, **96**, 1059–1078.

Marroni, M., Meneghini, F. & Pandolfi, L. 2017. A Revised Subduction Inception Model to Explain the Late Cretaceous, Double-Vergent Orogen in the Precollisional Western Tethys: Evidence From the Northern Apennines. *Tectonics*, **36**, 2227-2249.

Mével, C., Caby, R. & Kienast, J.R. 1978. Amphibolite facies conditions in the oceanic crust: example of amphibolized flaser-gabbro and amphibolites from the Chenaillet ophiolite massif (Hautes Alpes, France). *Earth and Planetary Science Letters*, **39**, 98–108.

Michard, A., Goffe, B., Chopin, C. & Henry, C. 1996. Did the Western Alps develop through an Oman-type stage? The geotectonic setting of high-pressure metamorphism in two contrasting Tethyan transects. *Eclogae Geologicae Helvetiae,* **89**, 43-80.

Miranda, E.A. & Dilek, Y. 2010. Oceanic core complex development in modern and ancient oceanic lithosphere: Gabbro-localized versus peridotite-localized detachment models. *Journal of Geology* **118**, 95-109, https://doi: 10.1086/648460.

Odin, G.S. 1994. Geological time scale. *Académie des Sciences Comptes Rendus*, ser. II, **318**, 59–71.

Oner, Z. & Dilek, Y. 2013. Fault kinematics in supradetachment basin formation, Menderes core complex of western Turkey. *Tectonophysics*, **608**, 1394-1412. DOI: 10.1016/j.tecto.2013.06.003

Pálfy, J., Smith, P.L., & Mortensen, J.K. 2000. Au-Pb and ^{40}Ar–^{39}Ar time scale for the Jurassic. *Canadian Journal of Earth Sciences*, **37**, 923-944.

Pandolfi, L. & Marroni, M. 1996. Litostratigrafia ed assetto strutturale delle unità Liguri Interne nel settore dell'alta val Trebbia ed alta val d'Aveto (Appennino Ligure). *Bollettino della Società Geologica Italiana*, **115**, 673-688.

Pearce, J.A. 2014. Immobile element fi ngerprinting of ophiolites. *Elements*, **10**, 101-108.

Pearce, J.A. & Robinson, P.T. 2010. The Troodos ophiolitic complex probably formed in a subduction initiation, slab edge setting. *Gondwana Research*, **18**, 60-81.

Perez-Guissinye, M. & Reston, T. J. 2000. Rheological evolution during extension at nonvolcanic rifted margins: Onset of serpentinization and development of detachments leading to continental breakup. *Journal of Geophysical Research*, **106**, 3961-3976.

Pinet, N., Lagabrielle, Y. & Whitechurch, H., 1989. Le complexe du Pic des Lauzes (Haut Queyras, Alpes Occidentales, France): structures alpines et océaniques dans un massif ophiolitique de type liguro-piémontais. *Bulletin de la Société géologique de France*, **2**, 317-326.

Philippot, P. 1990. Opposite vergence of nappes and crustal extension in the French-Italian Western Alps. *Tectonics,* **9** (5), 1143–1164.

Piccardo, G. 2009. Evolution of the lithospheric mantle in an extensional setting: Insights from ophiolitic peridotites. *Lithosphere*, **1**, 81-87.

Piccardo, G. B. & Guarnieri, L. 2010. Alpine peridotites from the Ligurian Tethys: an updated critical review. *International Geology Review*, **52**, 1138–1159.

Piccardo, G. B., Padovano, M. & Guarnieri, L. 2014. The Ligurian Tethys: mantle processes and geodynamics. *Earth-Science Reviews*, **138**, 409-434.

Péron-Pinvidic, G. and Manatschal, G. 2009. The final rifting evolution at deep magma-poor passive margins from Iberia-Newfoundland: a new point of view. *International Journal of Earth Sciences*, **98**, 1581-1597.

Platt, J.P., Behrmann, J.H., Cunningham, P.C., Dewey, J.F., Helman, M., Parish, M., Shepley, M.G., Wallis, S. & Western, P.J. 1989. Kinematics of the Alpine arc and the motion history of Adria. *Nature*, **337**, 158–161, doi: 10.1038/337158a0

Pognante, U., Perotto, A., Salino, C. & Toscani, L. 1986. The ophiolitic peridotite of the western Alps: Record of the evolution of a small oceanic-type basin in the Mesozoic Tethys. *Tschermaks Mineralogische und Petrographische Mitteilungen*, **35**, 47-65.

Polino, R., Dal Piaz, G.V. & Gosso, G. 1990. Tectonic erosion at the Adria margin and accretionnary processes for the Cretaceous orogeny of the Alps. *Mémoire de la Société Géologique de France,* **156**, 345-367.

Principi, G., Bortolotti, V., Chiari, M., Cortesogno, L., Gaggero, L., Marcucci, M., Saccani, E. & Treves, B. 2004. The pre-orogenic volcano-sedimentary covers of the western Tethys oceanic basin: a review. *Ofioliti*, **29**,177–212.

Rebay, G., Zanoni, D., Langone, A., Luoni, P., Tiepolo, M. & Spalla, M.I. 2018. Dating of ultramafic rocks from the Western Alps ophiolites discloses Late Cretaceous subduction ages in the Zermatt-Saas Zone. *Geological Magazine*, **155**(2), 298-315.

Ricou, L. E. & Siddans, W. B. 1986. Collision tectonics in the western Alps. *In* Coward M. P. & Ries L.E. (Eds), Collision Tectonics, Geological Society, London, Special Publication, **19**, 229–244.

Rosenbaum, G. & Lister, G.S. 2005. The Western Alps from the Jurassic to Oligocene: spatio-temporal constraints and evolutionary reconstructions. *Earth-Sciences Review,* **69**, 281-306.

Rubatto, D. & Angiboust, S. 2015. Oxygen isotope record of fluid metasomatism during subduction: a P-T-time-fluid path for the Monviso eclogites (Italy). *Contributions to Mineralogy and Petrology,* **170**(44).

Rubatto D., Gebauer D. & Fanning M. 1998. Jurassic formation and Eocene subduction of the Zermatt-Saas-Fee ophiolites: Implications for the geodynamic evolution of the Central and Western Alps. Contributions to Mineralogy and Petrology, **132**, 269–287.

Rubatto, D. & Hermann, J. 2003. Zircon formation during fluid circulation in eclogites (Monviso, Western Alps): implications for Zr and Hf budget in subduction zones. *Geochimica et Cosmochimica Acta,* **67** (12), 2173–2187.

Saby, P. 1987. La lithosphere oceanique de la Tethys ligure: etude du magmatisme et des mineralisations associees dans les ophiolites du Queyras (zone piemontaise des Alpes occidentales). Geologie appliquee Universite Scientique et Medicale de Grenoble, PHD Thesis.

Saccani, E., Dilek, Y., Marroni, M. & Pandolfi, L. 2015. Continental margin ophiolites of Neotethys: Remnants of Ancient Ocean-Continent Transition Zone (OCTZ) lithosphere and their geochemistry, mantle sources and melt evolution patterns. *Episodes*, **38**, 230–249.

Saccani, E., Dilek, Y. & Photiades, A. 2018. Time-progressive mantle-melt evolution and magma production in a Tethyan marginal sea: A sase study of the Albanide-Hellenide ophiolites. *Lithosphere* **10**, 35-53, doi: 10.1130/L602.1.

Schaaf, A., Polino, R., & Lagabrielle, Y. (1985). Nouvelle de´couverte de radiolaires d'aˆge Oxfordien supérieur-Kimméridgien inférieur à la base d'une série supra-ophiolitique des schistes lustrés piémontais (Massif de Traversiera, Haut Val Maıra, Italie). *Comptes Rendus de l'Académie des Sciences*, Paris, **14**(II), 1079–1084.

Schwartz, S., Guillot, S., Reynard, B., Lafay, R., Nicollet, C., Debret, B. & Auzende, A.L. 2013. Pressure–temperature estimates of the lizardite/antigorite transition in high pressure serpentinites. *Lithos*, **178**, 197-210, doi:10.1016/j.lithos.2012.11.023.

Shallo, M. & Dilek, Y. 2003. History of development of the ideas on the origin of the Albanian ophiolites. In, Dilek Y & Newcomb, S. (Editors), *Ophiolite Concept and the Evolution of Geological Thought, Geological Society of America Special Paper* **373**, 351-364.

Smith, T.L. & Batiza, R. 1989. New field and laboratory evidence for the origin of hyaloclastite flows on seamount summits. *Bulletin of Volcanology,* **51**(2), 96-114.

Stampfli, G.M. & Marthaler, M. 1990. Divergent and convergent margins in the North-Western Alps confrontation to actualistic models. *Geodinamica Acta*, **4**, 159-184.

Steinmann, G. 1905. Geologische beobachtungen in den Alpen, II. Die Schardtsche Ueberfaltungstheorie und die geologische Bedeutung der Tiefseeabsätze un der ophiolithischen Massengestein. Berichte der Naturforschenden Gesellschaft zu Freiburg im Breisgau, 16, 18-67.

Steinmann, G. 1927. Die ophiolitischen Zonen in den mediterranen Kettengebirgen (The Ophiolitic zones in the Mediettarean mountain chains). 14th International Geological Congress in Madrid, 2, 638-667.

Steck, A & Hunziker, J. 1994. The tertiary structural and thermal evolution of the Central Alps: compressional and extensional structures in an orogenic belt. *Tectonophysics*, **238**, 229–254.

Tankut, A., Dilek, Y. & Önen, P. 1998. Petrology and geochemistry of the Neo-Tethyan volcanism as revealed in the Ankara Mélange, Turkey. *Journal of Volcanological & Geothermal Research*, **85** (1/4), 265-284.

Tartarotti, P., Festa, A., Benciolini, L. & Balestro, G. 2017. Record of Jurassic mass transport processes through the orogenic cycle: Understanding chaotic rock units in the high pressure Zermatt-Saas ophiolite (Western Alps). *Lithosphere*, **9**(3), 399-407. doi:10.1130/L605.1

Tribuzio, R., Garzetti, F., Corfu, F., Tiepolo, M. & Renna, M. R. 2016. U–Pb zircon geochronology of the Ligurian ophiolites (Northern Apennine, Italy): Implications for continental breakup to slow seafloor spreading. *Tectonophysics*, **666**, 220–43.

Tricart, P. 1973. Tectoniques superposées dans les calcschistes piémontais du Haut-Cristillan (Queyras, Alpes franco-italiennes). *Comptes Rendus de l'Académie des Sciences*, **76**, 705-708.

Tricart P. & Lemoine M. 1983. Serpentinite oceanic bottom in South Queyras ophiolites (French Western Alps): record of the incipient oceanic opening of the mesozoic ligurian Tethys. *Eclogae Geologie Helvetiae*, **76**(3), 611-629.

Tricart, P. & Lemoine, M. 1991. The Queyras ophiolite west of Monte Viso (Western Alps): indicator of a peculiar ocean floor in the Mesozoic Tethys. *Journal of Geodynamics,* **13**, 163–181.

Tricart, P. & Schwartz, S. 2006. A north-south section across the Queyras Schistes lustrés (Piedmont zone, western Alps): Syn-collision refolding of a subduction wedge. *Eclogae Geologicae Helvetiae,* **99**, 429–442.

Tucholke, B., Lin, J. & Kleinrock, M.C. 1998. Megamullions and mullion structure defining oceanic metamorphic core complexes on the Mid-Atlantic Ridge. *Journal of Geophysical Research,* **103**, 9857-9866.

Vissers, R.L.M., Van Hinsbergen, D.J.J., Meijer, P.TH. & Piccardo, G.B. 2013. Kinematics of Jurassic ultra-slow spreading in the Piemonte Ligurian ocean. *Earth and Planetary Science Letters,* **380**, 138–150.

Vitale Brovarone, A., Picatto, M., Beyssac, O., Lagabrielle, Y., & Castelli, D., 2014. The blueschist-eclogite transition in the Alpine chain: P-T paths and the role of slow-spreading extensional structures in the evolution of HP-LT mountain belts. *Tectonophysics,* **615-616***,* 96-121.

Yu, Z., Li, J., Liang, Y., Han, X., Zhang, J & Zhu, L. 2013. Distribution of large-scale detachment faults on mid-ocean ridges in relation to spreading rates. *Acta Oceanologica Sinica*, **32**(12), 109-117, https://doi.org/10.1007/s13131-013-0397-y.

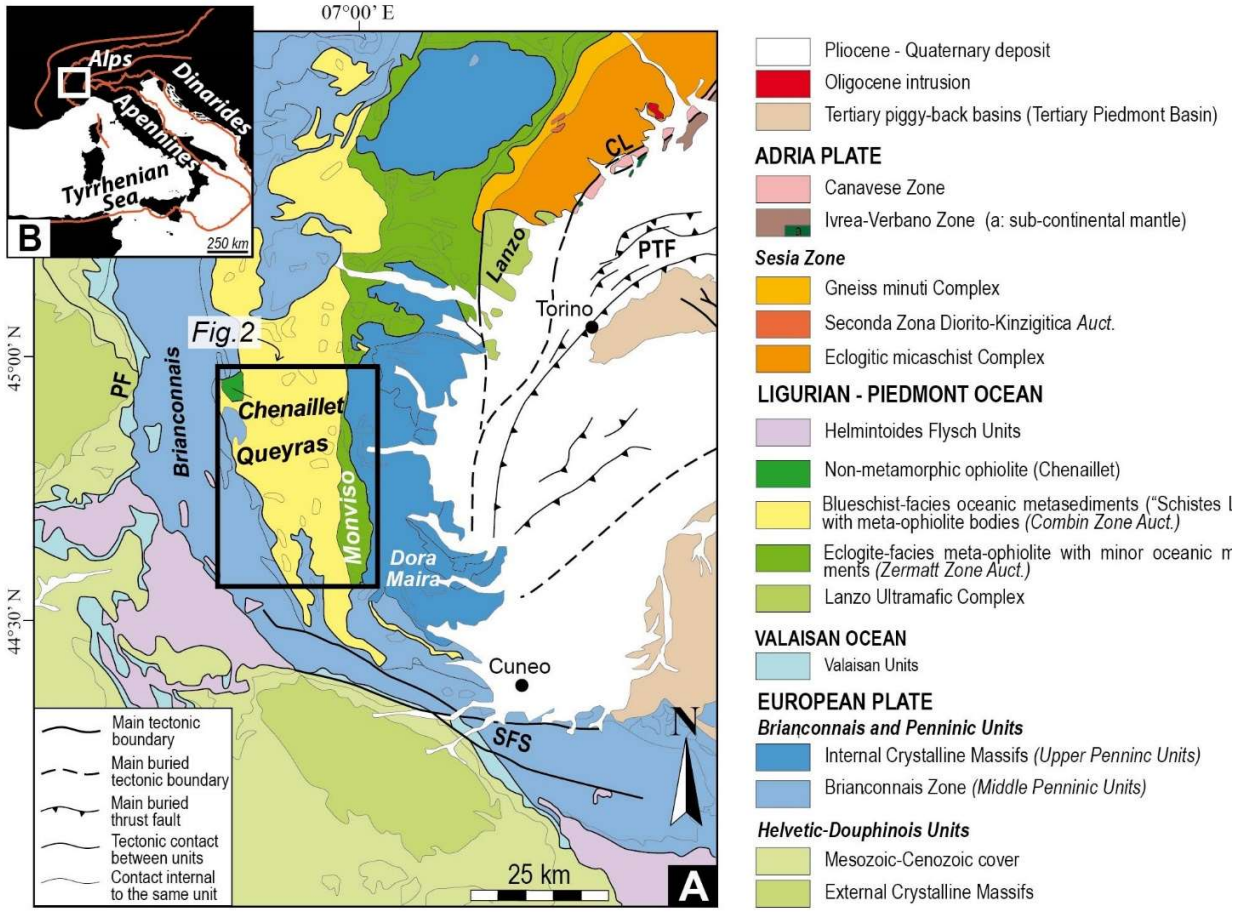

Figure 1 – (**A**) Simplified tectonic map of the Western Alps (modified from Balestro et al., 2015b) showing the location of the study area (black rectangle) (CL: Canavese Line; PF: Penninic Front; PTF: Padane Thrust Front; SFS: Stura Fault System). (**B**) Location of the Western Alps within the broader Alpine orogenic belt.

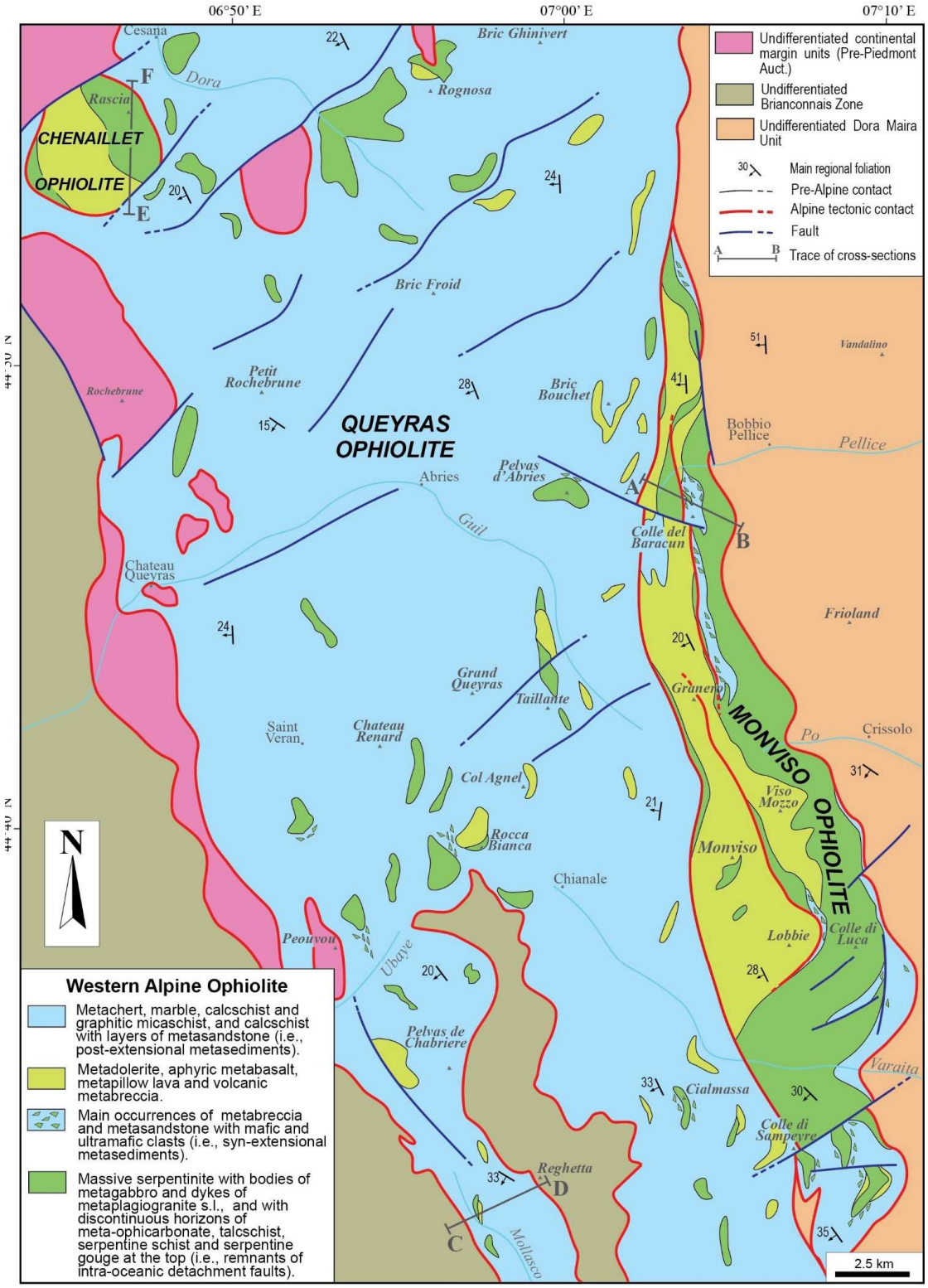

Figure 2 – Geological map of the study area in the Western Alps, showing the spatial and tectonic relationships between the Monviso, Queyras and Chenaillet ophiolites, and the continental margin units of Europe (modified from Balestro et al., 2011, 2013, 2018; Kerckhove et al., 1979).

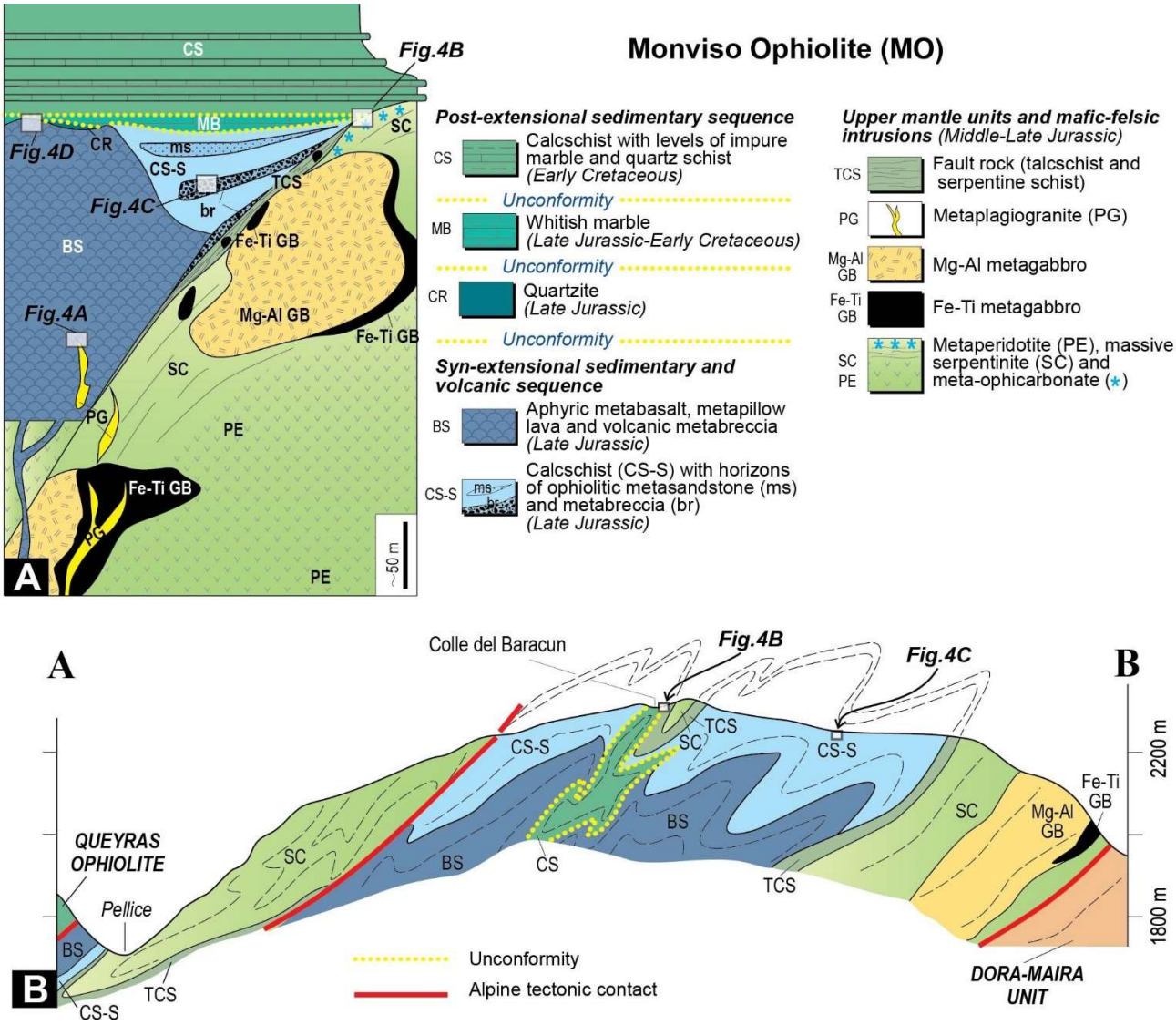

Figure 3 – (**A**) Pre-alpine stratigraphic columnar section of the Monviso ophiolite, depicting the lateral and vertical variations in the ophiolite and the overlying sedimentary succession. The sharp tectonic contact between the mantle-gabbro rocks and the syn-extensional volcanic and sedimentary rocks represent the Baracun Shear Zone (Festa et al. 2015), an intra-oceanic detachment fault marked by the occurrence of talcschist and serpentine schist. (**B**) Representative geological cross-section of the present-day structural and geological setting of the Monviso ophiolite (cross section profile is shown in Figure 2).

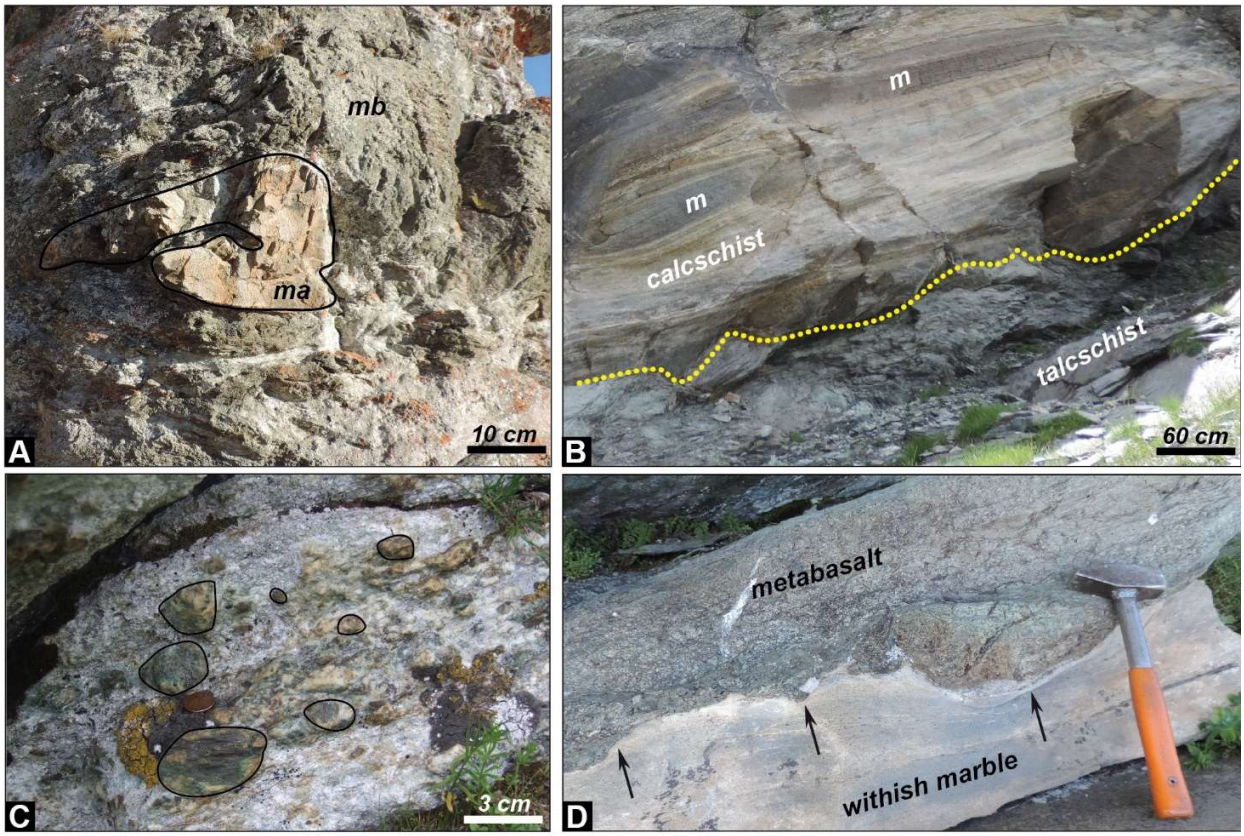

Figure 4 – Field images of various lithologies and contact relationships in the Monviso ophiolite: **(A)** Folded meta-albitite (ma) dyke (black line) intrusion in metabasalt (mb) (E of Colle di Sampeyre, Long. 7°8'48, Lat. 44°32'18); **(B)** Talcschist-bearing detachment fault, unconformably overlain (dotted yellow line) by post-extensional calcschist with impure marble (m) horizons (Colle del Baracun, Long. 7°3'50, Lat. 44°46'32); **(C)** Close-up image of a syn-extensional metabreccia, consisting of gabbroic clasts (black lines) in a coarse-grained mafic matrix (E of Colle del Baracun, Long. 7°4'11, Lat. 44°46'26); **(D)** Overturned primary contact (black arrows) between metabasalt and post-extensional whitish marble (SE of Colle di Luca, Long. 7°9'25, Lat. 44°37'24; hammer for scale).

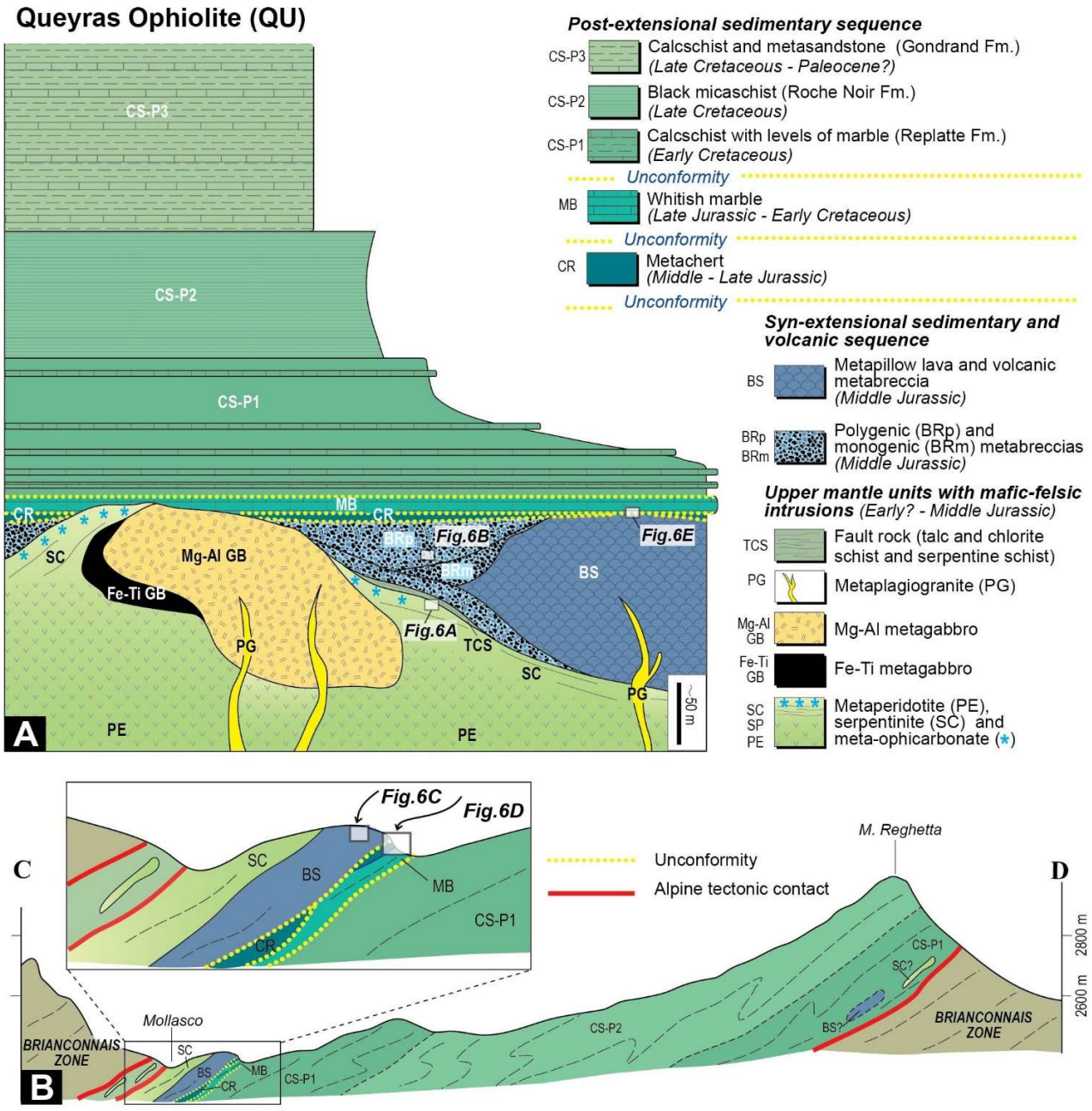

Figure 5 – (**A**) Pre-alpine stratigraphic columnar section of the Queyras ophiolite, depicting the lateral and vertical variations in the ophiolite and the overlying sedimentary succession. Talc and chlorite schist and serpentine schist marking a shear zone (TCS) between the UM peridotites–gabbros and the syn-extensional lavas and metasediments, interpreted as a low–angle detachment fault (see also Lagabrielle et al., 2015). (**B**) Representative cross section of the present-day structural and geological setting of the Queyras ophiolite (cross section profile is shown in Figure 2).

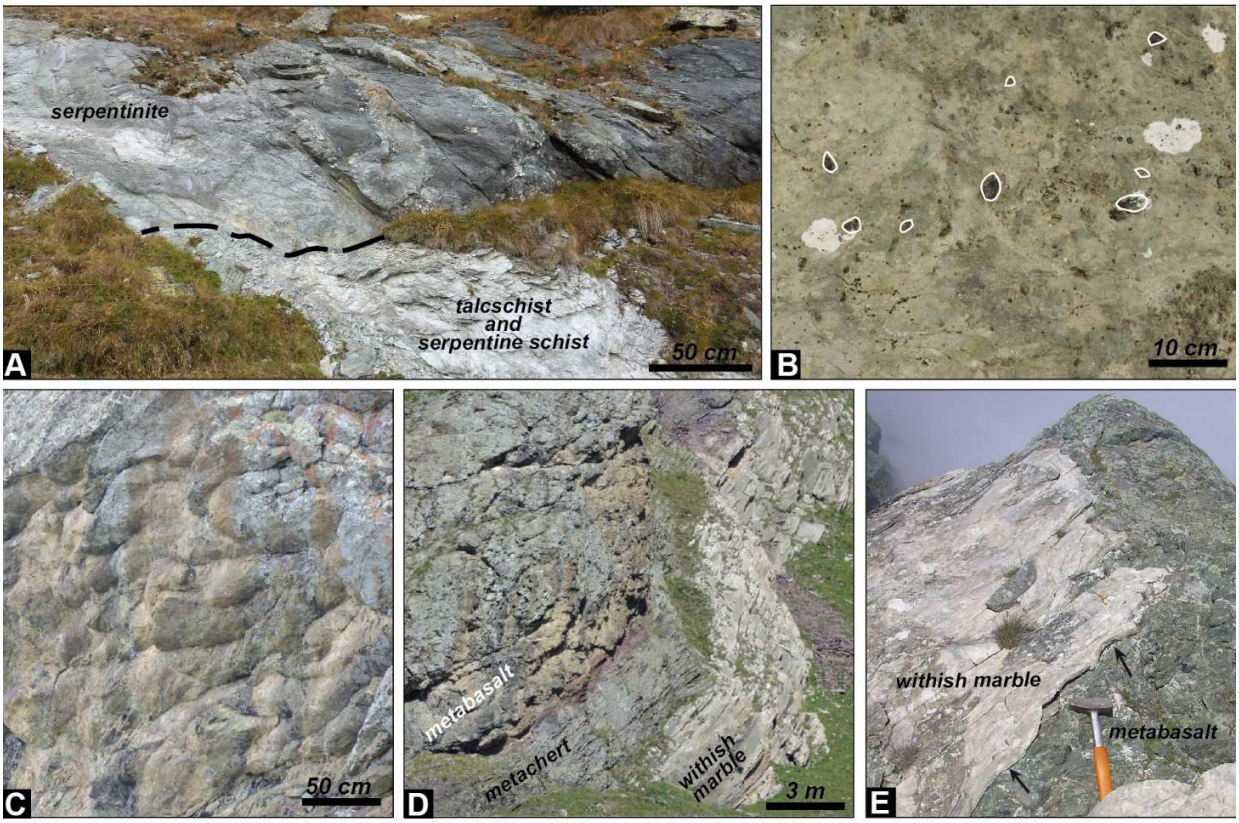

Figure 6 – Field images of various lithologies and contact relationships in the Queyras ophiolite: **(A)** The dashed line between the massive serpentinite and talcschist–serpentine schist marks a tectonic contact. Talcschist – serpentine schist is part of an extensional shear zone (detachment fault) (E of Cialmassa, Long. 7°6'22, Lat. 44°33'19); **(B)** Close-up photograph of syn-extensional metasandstone, consisting of serpentinite clasts (white lines) in a fine-grained carbonate matrix (Cialmassa, Long. 7°5'45, Lat. 44°33'34); **(C)** Close up view of preserved metapillow lavas in the syn-extensional volcanic sequence (Mollasco, Long. 6°57'9, Lat. 44°31'46); **(D)** Overturned primary contact between the metabasalt, metachert and whitish marble units (Mollasco, Long. 6°57'9, Lat. 44°31'46). **(E)** Primary unconformity contact (black arrows) between the metabasalt unit and the post-extensional whitish marble (SE of Bric Bouchet, Long. 7°1'16, Lat. 44°47'58; hammer for scale).

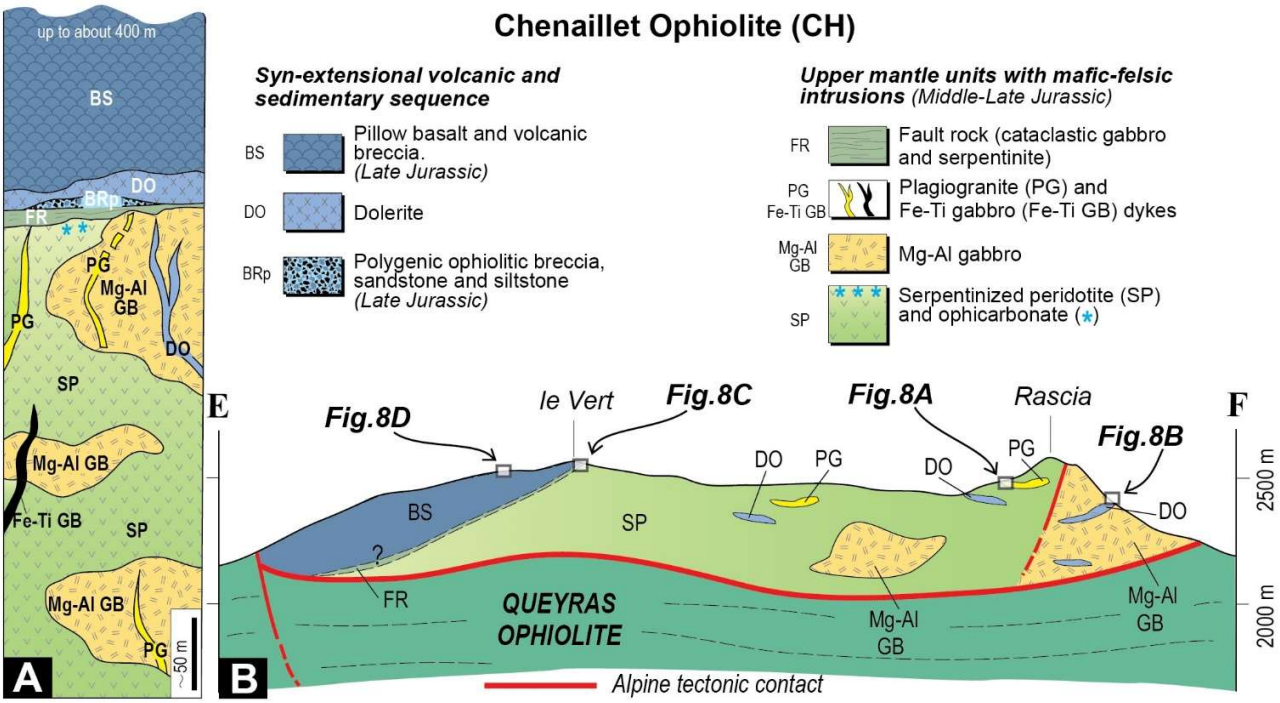

Figure 7 – (**A**) Pre-Alpine stratigraphic columnar section of the Chenaillet ophiolite, depicting the contact relationships between the UM peridotites, gabbros, various dyke intrusions, basaltic lavas, volcanic breccia and syn-extensional sediments (modified after Manatschal et al., 2011). Fault rocks (FR) mark the inferred detachment fault (Manatschal et al., 2011). (**B**) Representative cross section of the present-day structural and geological setting of the Chenaillet ophiolite (cross section profile is shown in Figure 2).

Figure 8 – Field images of various lithologies and contact relationships in the Chenaillet ophiolite: **(A)** Albitite dyke intrusion in a serpentinized peridotite (S of Punta Rascia, Long. 6°46'50, Lat. 44°55'30; hammer for scale); **(B)** Close-up view of a dolerite dyke intruded into a Mg-Al gabbro (Punta Rascia, Long. 6°46'37, Lat. 44°55'48); **(C)** Primary contact (dashed white line) between a basaltic lava flow on top and a cataclastically deformed serpentinite below. This cataclastic serpentinite is part of an extensional shear zone and detachment fault (hammer for scale) (Cima le Vert, Long. 6°46'31, Lat. 44°54'41); **(D)** Basaltic pillow lava flows (W of Cima le Vert, Long. 6°46'26, Lat. 44°54'33).

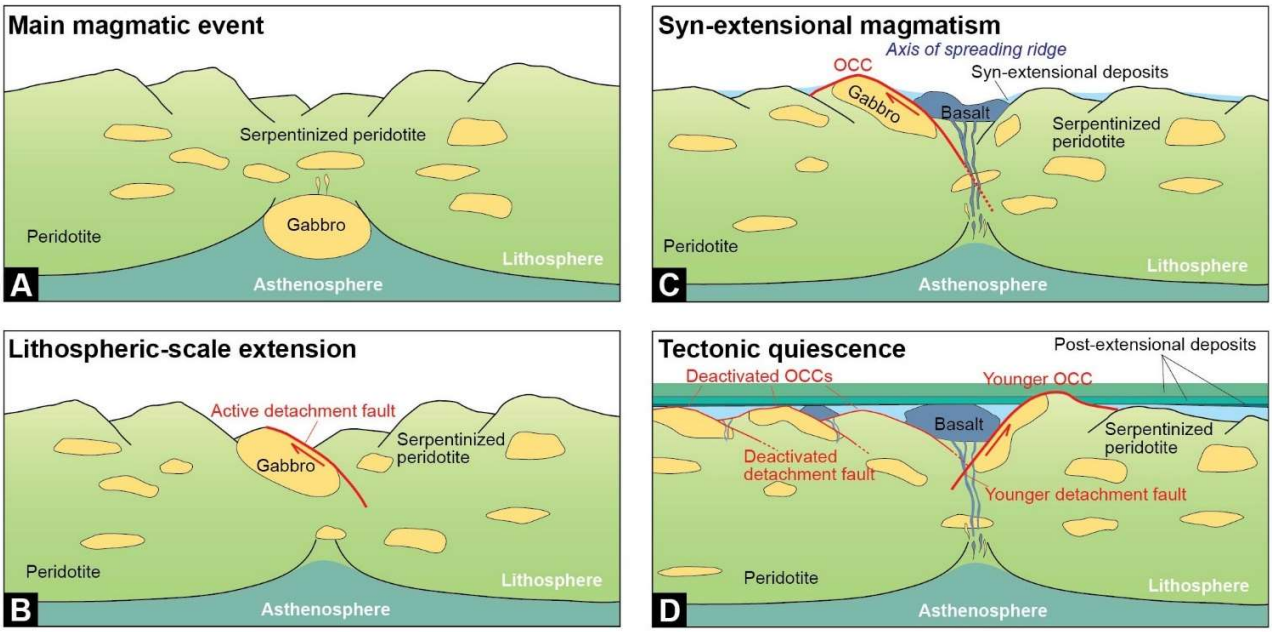

Figure 9 – Sequential tectonic diagrams depicting the four main stages of the evolution of the WAO emplacement (modified from Ildefonse et al., 2007). (**A**) Main magmatic event (Stage 1), (**B**) Lithospheric-scale extension and UM exhumation controlled by detachment faulting (Stage 2), (**C**) Syn-extensional volcanism and sedimentation on the exhumed detachment fault and UM peridotites (Stage 3). This stage corresponds to the seafloor spreading and oceanic core complex development episode along a slow-spreading ridge system within the LPO. (**D**) Tectonic quiescence phase and deposition of the post-extensional sedimentary sequence (Stage 4).

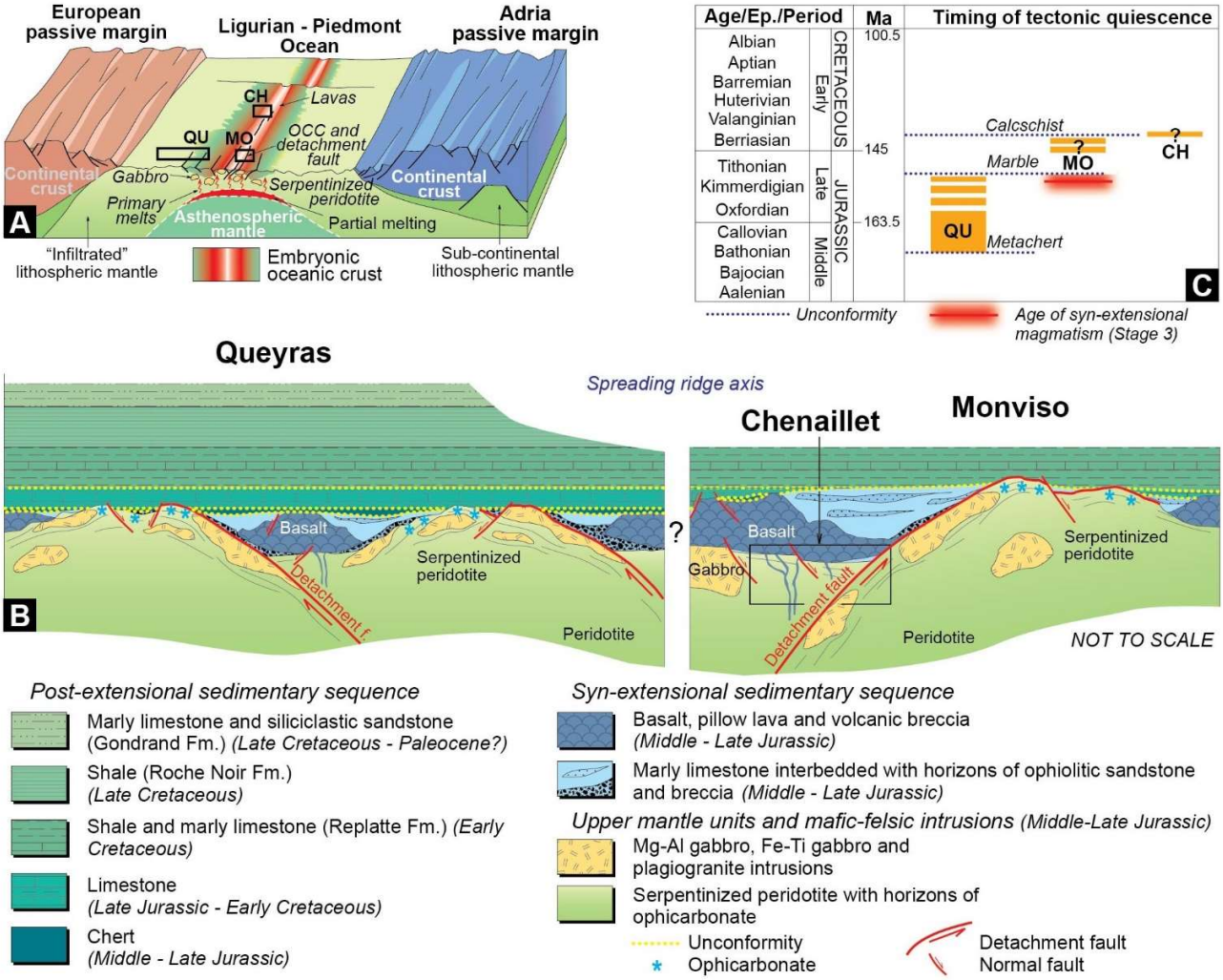

Figure 10 – (**A**) Interpretative block diagram depicting the inferred palaeogeography of the Ligurian–Piedmont Ocean and the rifted continental margins of Europe and Adria (modified from Balestro et al., 2018; Frontal cross-section modified from Dilek & Furnes, 2011; Piccardo, 2009; Peron-Pinvidic & Manatschal, 2009). (**B**) Simplified reconstruction of the seafloor architecture of the WAO, as preserved after the sealing of the post-extensional succession. The sedimentary cover shows lateral and vertical variations, passing from a complete succession in the Queyras ophiolite to a reduced succession in the Monviso ophiolite. (**C**) Time chart showing a diachronous development of the tectonic quiescence phase (Stage 4), across the WAO and the LPO, as inferred from the timing of the main unconformities sealing the exhumed UM rocks (see text for details). Timing of the syn-extensional magmatism (Stage 3) is also marked for the Monviso ophiolite (red bar). Dashed orange bars represent inferred ages. Time scale adopted from Cohen et al. (2013).